The University of Alberta
Printing Department
Edmonton, Alberta

THE UNIVERSITY OF ALBERTA

AEROFOILS AT LOW REYNOLDS NUMBER

BY

ROGER THOMAS ARGUMENT

A THESIS

SUBMITTED TO THE FACULTY OF GRADUATE STUDIES

IN PARTIAL FULFILMENT OF THE REQUIREMENTS FOR THE DEGREE

OF MASTER OF SCIENCE

DEPARTMENT OF MECHANICAL ENGINEERING

EDMONTON, ALBERTA

SPRING, 1971

UNIVERSITY OF ALBERTA

FACULTY OF GRADUATE STUDIES

The undersigned certify that they have read, and recommend to the Faculty of Graduate Studies for acceptance, a thesis entitled "AEROFOILS AT LOW REYNOLDS NUMBERS" submitted by ROGER THOMAS ARGUMENT in partial fulfilment of the requirements for the degree of Master of Science.

ABSTRACT

This thesis was undertaken to examine the available information on the operation of aerofoils at low Reynolds numbers with a view to determining the best currently available aerofoil sections for use at low Reynolds numbers.

The comparison was based upon a study of the maximum lift coefficient, the minimum drag coefficient and $(C_L/C_D)_{max}$ of the various aerofoils. Results showed the aerofoils specifically designed for low Reynolds number operation possess better aerodynamic characteristics than conventional aerofoils.

Recommendations are made where it is felt that further research would be useful.

ACKNOWLEDGEMENTS

The author would like to express his appreciation to Dr. D. J. Marsden for his guidance and supervision. Thanks also go to Miss Helen Wozniuk for the typing of this thesis. The financial assistance of the National Research Council of Canada and the University of Alberta is appreciated. Last of all, he would like to thank his wife, Carol, for her support.

TABLE OF CONTENTS

TABLE OF CONTENTS (continued)

LIST OF FIGURES

LIST OF FIGURES (continued)

NOTATION

c	chord length
C_D	section drag coefficient
C_f'	dimensionless local skin friction coefficient
C_L	section lift coefficient
C_P	pressure coefficient
K	height of roughness element
o	as a subscript - indicates conditions at the leading edge
P	pressure
q	dynamic pressure
Re	Reynolds number
R_K	Reynolds number based on grain size
R_x	Reynolds number based on distance from leading edge
R_{xr}	Reynolds number of transition - rough plate
R_{xs}	Reynolds number of transition - smooth plate
t_r	as a subscript - indicates conditions at the transition position
U	magnitude of potential flow velocity
U', U''	first and second derivatives of potential flow velocity with respect to x
u,v,w	velocities in the three coordinate directions
x,y,z	the three coordinate directions
δ	boundary layer thickness
δ_K	displacement boundary layer thickness at roughness element
Λ	shape factor

NOTATION (continued)

μ	absolute viscosity
ν	kinematic viscosity
ρ	density
σ	turbulence level

CHAPTER I

INTRODUCTION

B.S. Shenstone [1] described flight at Reynolds numbers less than 5×10^6 as "Unconventional Flight". He further defines it as "flight outside the mainstreams of research and development" and as flight that "shows itself to be restricted to the low Reynolds numbers."

There are many applications for aerofoils operating at Reynolds numbers below 5×10^6. Some of these are: fans and turbines, helicopter blades, propeller blades, light aircraft and sailplanes, windmills, and model aircraft.

That the great concentration of research and development is at the higher end of the Reynolds number scale is common knowledge. As military and commercial aircraft steadily increase in size and speed, the emphasis is not likely to change.

The intensive investigations that are devoted to the understanding of the phenomena that occur in the boundary layer of compressible flow are in response to the rapid increase in the flying speeds of modern aircraft [2]. Compressible flow is generally understood to mean flight at speeds in excess of approximately 300 miles per hour. For an aerofoil with a chord of 4 feet at an altitude of 2000 feet above sea level, this speed corresponds to a Reynolds number of approximately 11×10^6.

The above considerations imply that the development of low

Reynolds number aerofoils will lag behind the development of conventional aerofoils. Shenstone says that any work at all is solely due to a few talented and enthusiastic people with a personal interest in the field. Accordingly, one would expect that the amount of available information on low Reynolds number aerofoils to be quite small. One would also expect that in some cases a high Reynolds number aerofoil might be used in a low Reynolds number application where it would perform badly, the poor choice of aerofoil section having been made simply because of a lack of information and reliable test data on aerofoils at low Reynolds numbers.

To give one example, the flat-bottomed Clark Y, or an aerofoil resembling it, is the section commonly used in fans [3]. It is shown later that this aerofoil is by no means as efficient as others that are now available.

The purpose of this thesis is to survey the available information on the operation of aerofoils at low Reynolds numbers in order to compare the performance of currently available aerofoil sections and to outline areas where further research would be useful.

The bulk of the study is made of three main parts. Chapter II gives a brief qualitative discussion of the factors that affect low Reynolds number flow. Chapter III discusses the available information on conventional aerofoils at low Reynolds numbers and indicates which of these appear to be most promising. Chapter IV presents the work done on aerofoils specifically designed for low Reynolds numbers. The

best aerofoils in this group are also indicated.

Some recommendations are made, based on a comparison of the data presented in this thesis.

CHAPTER II

BOUNDARY LAYER CONSIDERATIONS

The complications that arise in designing an aerofoil for low Reynolds number applications are considerably more numerous than those met at high Reynolds numbers. The fact that the Reynolds number is low means that phenomena such as laminar boundary layer separation and transition to turbulence are highly variable and difficult to account for adequately. At high Reynolds numbers, these phenomena are not so much of a problem. The higher Reynolds number flows experience earlier transition to turbulence and this eliminates laminar boundary layer separation, although turbulent boundary layer separation may still occur.

This chapter provides some explanation of the factors that affect low Reynolds number flow. The effect of pressure gradients, both favourable and adverse, on laminar and turbulent boundary layers are discussed. The effect of surface roughness is discussed briefly.

2.1 Laminar Separation

Consider the flow on the suction side of an aerofoil. The flow initially experiences a reduction in pressure as the velocity increases over the forward part of the aerofoil. This is in accordance with Bernoulli's equation:

$$P + \frac{1}{2} \rho U^2 = \text{constant} .$$

The pressure at the trailing edge of the aerofoil is higher than the minimum pressure over the aerofoil. Pressure recovery over the rear part of the aerofoil results in an adverse pressure gradient, as is illustrated in Figure 2-1.

The phenomenum of separation occurs when a boundary layer encounters an adverse pressure gradient [4]. The boundary layer flow just slightly above the surface over which the flow moves is known to be much slower than the free stream flow and, accordingly, the momentum of a fluid particle just above the surface is relatively low. When an adverse pressure gradient is impressed upon the boundary layer flow, these low momentum fluid particles are slowed down. They may be brought to a standstill or be forced to flow in an upstream direction. Separation has then occurred.

It has been shown [2] that laminar flows can support only very small adverse pressure gradients without experiencing separation. Therefore adverse pressure gradients that exist in the flow over an aerofoil can be expected to cause separation, or transition to turbulence if the Reynolds number is high enough. Later, in Section 2.3, it will be shown that a turbulent flow can resist separation in the face of considerably stronger adverse pressure gradients than can laminar flows.

Without resorting to active methods of boundary layer control such as suction or blowing, the only way to prevent separation of a laminar boundary layer is to require that the adverse pressure gradient remain below the limit for separation. Prandtl has shown how it is

possible to estimate this limiting pressure gradient [2].

The Kármán-Polhausen approximate method for the solution of two dimensional boundary layer flows with pressure gradient can be used to show that when a flow is approaching a separation condition, a dimensionless quantity, Λ, is decreasing numerically through the value of -12 [2]. The dimensionless quantity, Λ, called the shape factor, is written as

$$\Lambda = \frac{\delta^2}{\nu}\frac{dU}{dx} \text{ or } \Lambda = -\frac{dP}{dx}\frac{\delta}{\mu\frac{U}{\delta}},$$

and is physically interpreted as the ratio of pressure forces to viscous forces.

Figure 2-2 shows the dimensionless x-direction velocity, u/U, versus the dimensionless vertical distance, $\eta = y/\delta$, above the plate for various values of Λ. When Λ has the value -12,

$$\left(\frac{\partial u}{\partial y}\right)_{y=0} = 0,$$

and since the no-slip boundary condition says that

$$(u)_{y=0} = 0,$$

the flow is just on the verge of reversing direction near the plate.

To keep the flow just below the separation point, Prandtl chose $\Lambda = -10$ and showed that this value corresponded to

$$\frac{UU''}{(U')^2} \simeq 11 \qquad (2\text{-}1)$$

where

$$\frac{UU''}{(U')^2} > 11 \text{ and } \frac{UU''}{(U')^2} < 11$$

implied no separation and separation respectively.

The above equation (2-1) can be integrated after rearranging as

$$\frac{U''}{U'} = 11 \frac{U'}{U} \ .$$

Repeated integration yields

$$\frac{U^{-10}}{10} = C_1 x + C_2 \ .$$

After the constants are determined, the potential flow velocity can be written as

$$U(x) = \frac{U_o}{\left(1 + 100 \frac{\nu x}{U_o \delta_o^2}\right)^{1/10}} \qquad (2\text{-}2)$$

where U_o and δ_o are respectively, the potential flow velocity and the boundary layer thickness just prior to the separation point.

The momentum equation for flow over a flat plate is

$$u \frac{\partial u}{\partial x} + v \frac{\partial u}{\partial y} = - \frac{1}{\rho} \frac{\partial P}{\partial x} + \nu \frac{\partial^2 u}{\partial y^2} \quad .$$

In the region outside of the boundary layer, the free stream velocity, U(x), is a function of x only and the effect of viscosity is negligible. Therefore the momentum equation for the outer region becomes

$$U(x) \frac{dU(x)}{dx} = - \frac{1}{\rho} \frac{dP}{dx} \quad . \tag{2-3}$$

Using equation (2-3), the permissible pressure gradient is found to be

$$\frac{dP}{dx} = \frac{10 \mu U_o}{\delta_o^2} \frac{1}{\left(1 + \frac{100 \nu x}{U_o \delta_o^2}\right)^{6/5}}$$

From equation (2-2), the value of the permissible deceleration of the flow is seen to be small and is not very different from that of the case of constant velocity along a flat plate at zero incidence. Since such a case corresponds to constant pressure in the stream direction, it follows that the permissible adverse pressure gradient must be very small if separation of the laminar boundary layer is to be avoided.

At higher Reynolds numbers, however, laminar separations do not occur. For example, in reference [5], flow separations occurring on the NACA 66_3-018 were investigated and for Reynolds numbers greater

than 6×10^6, no separation takes place. Data on the same aerofoil at lower Reynolds numbers showed that the laminar boundary layer separated downstream of the suction peak. Apparently laminar separation has been avoided at the higher Reynolds numbers because of transition to turbulence in the boundary layer.

2.2 Transition

Although there is no complete understanding of the actual mechanism of transition from a laminar to a turbulent flow, a number of investigators including Tollmein, Schlichting, Lin, and others have shown that disturbances in a certain band of frequencies will tend to grow with time if the Reynolds number is above some specific minimum value [6]. These disturbances may originate from turbulence in the free stream, pressure waves, or surface roughness.

A list [6] of the parameters affecting transition contains the following entries; Reynolds number, pressure gradient, suction applied to the surface, free stream turbulence, surface roughness, surface curvature, heat addition or rejection, and compressibility. The most important of the parameters [2] are the pressure distribution in the free stream, surface roughness and the intensity of free stream turbulence.

The influence of the pressure distribution has been demonstrated by Schubauer and Skramstad[7]. A favourable pressure gradient delays transition while an unfavourable pressure gradient was found to encourage earlier transition. Laminar flow aerofoils, such as the NACA 6-series,

use the stabilizing effect of the favourable pressure gradient to achieve their low minimum drag coefficients.

Sometimes transition to turbulence is accomplished by separation of the flow. The separated shear layer will be laminar or turbulent, depending upon the Reynolds number. Laminar shear layers, however, are considerably more unstable than laminar boundary layers [4], and transition to turbulence has been observed at very low Reynolds numbers.

If the curvature of the body and the angle of incidence are not large, turbulent shear layers sometimes reattach to the surface as turbulent boundary layers [4], and thus, transition of the flow has been accomplished. Only a small region of separated flow exists and this region is called a separation bubble. On aerofoils, these separation bubbles have been observed to occur near both the nose of the aerofoil and near the mid chord position.

A study by Tani [8], based upon experimental results, has indicated that the formation of separation bubbles can be confined to a certain range of Reynolds numbers. For sufficiently high Reynolds numbers, the formation of a separation bubble will not occur because the transition point for the boundary layer will lie in front of the laminar separation point. For sufficiently low Reynolds numbers, the laminar shear layer will not turn turbulent and will not reattach itself. The range of Reynolds numbers over which separation bubbles occur is determined by factors such as the pressure distribution, surface roughness and free stream turbulence.

Generally, the presence of roughness favours transition by introducing additional disturbances into the laminar boundary layer. If the roughness elements are small enough however, the small disturbances produced will not be amplified and no effect upon transition results. For roughness elements of a certain size or larger, transition will take place right at the element location. Elements of intermediate sizes will produce transition at various distances downstream from the element.

The important factor is not the height of the roughness element alone but a combination of several factors that include the height of the roughness element, the stream velocity and pressure gradient.

Experimental investigations have been carried out on two types of roughness elements. One type is the single cylindrical two dimensional roughness element and the other type is distributed surface roughness. An example of the first type is a tripping wire, and of the second type, sand grains glued to the surface.

Extensive experimental work has been done for the two dimensional roughness elements. A typical curve of expected results, taken from reference [9], is shown in Figure 2-3. The ratio of K/δ_K is the ratio of the height of the roughness element to the displacement boundary layer thickness at the roughness element. The Reynolds number of transition of a smooth plate and of a rough plate are respectively denoted by R_{xs} and R_{xr}, both based on the position of transition.

For relatively small roughness elements, there is very little effect upon the point of transition but as the size of the roughness

element grows, relative to the displacement boundary layer thickness, the transition point moves steadily forward from the smooth plate transition point.

Schlichting [2] reports on one piece of experimental work done by E.G. Feindt on sand grain type roughness with pressure gradients. The results of Feindt's work are shown in Figure 2-4. The sand grain size is denoted by K. The density of the sand grains covering the surface is not mentioned. P_{tr} and P_o denote the pressure at the position of transition and at x = 0 respectively.

Figure 2-4 indicates that at first, for any given pressure gradient, the grain size has no effect upon the position of transition. Note that the more negative the pressure gradient, the higher the transition point Reynolds number. This follows from the work of Schubauer and Skramstad [7], who, as mentioned previously showed that a favourable pressure gradient delays transition. The grain size, however, does show an effect upon the transition point when the Reynolds number based on grain size, $R_K = UK/\nu$, increases beyond the approximate value of 120.

Riegels [10] reports upon some work done by Prandtl and Schlichting on the effect of sand grain type roughness on transition. Based on their work, a surface can be considered aerodynamically smooth if the Reynolds number based on grain size satisfies the relation,

$$\frac{UK}{\nu} \leq 100.$$

A similar study by Smith and Clutter [11] found that the height of roughness that first affected transition in laminar flow was given by

$$\frac{UK}{\nu} \simeq 40,$$

no matter what the pressure gradient was. The authors [11] decided, as "a factor of safety", to replace the value of 40 with 25. For $R_K < 25$, the flow is certain to remain laminar, for $R_K > 100$, transition to turbulence is ensured somewhere downstream of the roughness element. Another study by Clutter and mentioned in reference [12] showed that the first significant increase in drag occurs for

$$\frac{UK}{\nu} \simeq 100.$$

These two studies then are somewhat in agreement with the two earlier mentioned results of Feindt and Prandtl-Schlichting.

A relation for the calculation of the greatest admissible value of the roughness size is

$$K_{admiss} = \frac{5\nu}{U}\sqrt{\frac{2}{C_f}} \quad [12] \quad .$$

This relation is good for 2 or 3 dimensional flows, the existence or non-existence of pressure gradients, and laminar or turbulent flows.

The factor C_f' may be eliminated by using the relations:

$$C_f' = 0.0592\ (R_x)^{-1/5} \text{ and}$$

$$C_f' = 0.664\ (R_x)^{-1/2}$$

for turbulent and non-turbulent flow respectively[12]. Using these relations, the following expressions are obtained:

(1) for turbulent flow

$$\frac{K}{x} = 29\ R_x^{-0.9} \quad \text{or} \quad \frac{K}{c} = \frac{29}{R_c^{0.9}} \left(\frac{X}{c}\right)^{+0.1}$$

(2) for laminar flow

$$\frac{K}{x} = 8.68\ R_x^{-0.75} \text{ or } \frac{K}{c} = \frac{8.68}{R_c^{0.75}} \left(\frac{X}{c}\right)^{0.25} .$$

These relations were used in reference [12] to calculate the allowable roughness on two aerofoils and an elliptical body of revolution. The results of the calculations for the aerofoil NACA 64-415 at a $C_L = 0.4$ are shown in Figure 2-5.

The results are presented for three different Reynolds numbers based on the grain size. $R_K = 25$ corresponds to the value of K for which the flow is laminar, $R_K = 100$ corresponds to the value of K for which the transition will occur downstream, and $R_K = 400$ corresponds to

the value of K for which transition occurs at the element. Figure 2-5 shows that the maximum admissible roughness on the pressure surface is greater than that on the suction surface, due to the lower velocity on the pressure surface. Some comparisons were made of the maximum admissible roughness for a flat plate and an aerofoil. It was found that the admissible roughness on a flat plate is higher than it is on a body with favourable pressure gradients. This is directly opposed to the finding of Feindt shown in Figure 2-4.

As an illustration of the size of the roughness elements involved, consider the height of an element which will have no effect upon transition on the suction side of the NACA 64-415 at $C_L = 0.4$ and $R_e = 2.5 \times 10^6$. From Figure 2-5, this corresponds to $K/c = 5 \times 10^{-5}$ for $x/c = 0.05$. For an aerofoil with a 4 foot chord, this implies a height of 0.0024 inches, which is about as thick as a sheet of foolscap. This shows that great care must be taken to keep the aerofoil surfaces clean and smooth. A roughness element that will trigger transition downstream has a height of 0.0048 inches and immediate transition is triggered by an element of height 0.011 inches or greater.

Free stream turbulence is the last of the important parameters affecting transition as mentioned by Schlichting [2]. A commonly used measure of the turbulence of a stream involves the root-mean square value of the fluctuations. The parameter used as a measure of turbulence is,

$$\sigma = \frac{100}{U}\sqrt{\frac{1}{T}\int_0^T \frac{(u_1^2+v_1^2+w_1^2)}{3}\,dt}$$

where T is a relatively large length of time and u_1, v_1, and w_1 are the deviations of the x, y, z velocities from the mean velocities u, v, w. This gives a measure of the turbulence in terms of percent of the mean speed U where

$$U = (u^2 + v^2 + w^2)^{1/2} .$$

The effect of free stream turbulence upon laminar to turbulent transition was investigated by Schubauer and Skramstad [7] for the flat plate. A plot of their results is shown in Figure 2-6.

For low values of σ, there is no effect upon the Reynolds number of transition but as σ passes 0.09, the free stream turbulence begins to exert an effect, and the Reynolds number of transition is lowered.

2.3 Turbulent Separation

As mentioned in Section 2.1, separation may occur when a boundary layer encounters an adverse pressure gradient. Turbulent boundary layers are known to be more resistant to separation than are laminar boundary layers.

The curves shown in Figure 2-7 compare the turbulent velocity profile with the laminar profile of the same thickness. It shows that, for the turbulent case, the velocity near the surface is greater.

Therefore the turbulent boundary layer can be expected to drive further than the laminar boundary layer against an adverse pressure gradient.

Smith and Kaups [12] state that a turbulent boundary layer can withstand an adverse pressure gradient 2 or 3 times greater than that which will separate a laminar boundary layer.

CHAPTER III

CONVENTIONAL AEROFOILS

In the last forty to fifty years, there has been much work, both theoretical and experimental, to improve the performance of aerofoils used in conventional applications. The term conventional is used to denote aerofoils not specifically intended for low Reynolds number operation. There is abundant information available in the literature concerning the aerodynamic characteristics of such aerofoils. For example, numerous NACA Technical Notes and Technical Reports contain material related to the above mentioned topic.

These sources of information offer many comparisons and contrasts of different aerofoils. They show that aerofoil performance has reflected the attention given it, in that over the years, the performance of aerofoils has steadily improved. The most noticeable improvement in the important aerodynamic characteristics has been in the reduction of the drag coefficient. When laminar flow aerofoils, such as the NACA 6-series sections, were introduced, minimum drag coefficients reached significantly lower values than had previously been attained.

The effect of variations in the Reynolds number upon the maximum lift coefficient, the minimum drag coefficient and other important aerodynamic characteristics of these aerofoils has been extensively reported. The maximum lift coefficient increases and the

minimum drag coefficient decreases with increasing Reynolds number.

One thingthat the literature does not provide, however, is extensive information on aerodynamic characteristics of aerofoils at low Reynolds numbers. Even in relatively recent times, it has been found that lift and drag data for low Reynolds number aerofoils is scarce [3],[13]. A literature search has turned up only the following meager material on low Reynolds number tests of conventional sections.

3.1 Existing Experimental Data

Data concerning the performance of a single aerofoil, the 11.7% thick Clark Y, in the Reynolds number range 1.0×10^6 to 9.0×10^6 is contained in a report by Silverstein [14]. The large collection of aerodynamic data by Riegels [10] contains a small amount of information on some aerofoils at low Reynolds numbers. The low Reynolds number data is not very comprehensive on the aerofoils for which it is given, and the identification of trends in the aerofoil performance with varying Reynolds number is not possible. The largest collection of material on this topic appears in the study by Loftin and Smith [15]. This report contains experimental information on 15 NACA aerofoils tested at Reynolds numbers in the range 0.7×10^6 to 9.0×10^6.

Concern over the lack of information on aerodynamic data at low Reynolds numbers was the reason that this work was undertaken by Loftin and Smith. In the authors' words -

> "Although the range of Reynolds number covered by the investigations reported in reference [1]* is reasonably wide, engi-

---

*Abott, I.H., Von Doenhoff, A.E. and Stivers, L.S., Jr.: Summary of Airfoil Data, NACA Rep. 824, 1945.

> neering design problems such as may be encountered in the selection of wing sections for small personal-type airplanes may require data for a range of Reynolds number extending below 3×10^6."

It was felt that such a report would provide a basis upon which decisions could be made as to the best aerofoil type for low Reynolds number applications. Whether or not the authors considered designing and testing new aerofoils specifically intended for low Reynolds number applications is not mentioned.

The aerofoils investigated in reference [15] consisted of ten of the comparatively new NACA 6-series sections, two of the slightly older NACA 5-digit sections and three of the older yet NACA 4-digit sections. A list of the specific aerofoils chosen for the study is given below:

1. 64-409	6. 64_1A212	11. 23012
2. 64_1-412	7. 64_1-612	12. 23015
3. 64_2-415	8. 63_2-415	13. 0012
4. 64_3-418	9. 65_2-415	14. 4412
5. 64_1-012	10. 66_2-415	15. 4415

Numerous factors that could affect the aerodynamic characteristics of an aerofoil were investigated. The aerofoil thickness and the chordwise position of the minimum pressure were considered. The design lift of the aerofoils was considered. The effect of roughness on the aerodynamic characteristics was determined by performing the tests with both smooth and rough aerofoil surfaces. The influence of a flap upon the lift coefficient versus angle of attack curve was investigated.

Some of the conclusions of Loftin and Smith, based upon their experimental results are presented below in abbreviated form.

1. The minimum drag coefficient of all aerofoils, both rough and smooth, increased as the Reynolds number decreased. For smooth aerofoils, the increase was largest for the thickest aerofoils and for those aerofoils with the position of minimum pressure furthest back along the chord. For rough surfaced aerofoils and for smooth aerofoils at the lower Reynolds numbers, the minimum drag of the NACA 6-series sections was no better than that of the NACA 5-digit sections.

2. The width of the laminar bucket for the smooth NACA 6-series aerofoils increased with decreasing Reynolds number.

3. The maximum lift coefficient of all aerofoils decreased as the Reynolds number decreased.

4. The sharpness of the stall was decreased at low Reynolds number for those of the NACA 6-series sections that did show abrupt losses in lift at high Reynolds number. The NACA 230-series which stalled abruptly at high Reynolds numbers showed no improvement as the Reynolds number was lowered.

5. The lift curve slope for all aerofoils decreased somewhat with decreasing Reynolds number.

6. The value of the quarter-chord pitching moment at the design angle of attack did not vary with Reynolds number for the plain aerofoils.

3.2 Discussion of Data

Part of the data obtained in reference [15] has been used to produce the curves in Figures 3-1 and 3-2. Data for the Clark Y was ob-

tained from reference [14]. Some comments can be made as to the best type of conventional aerofoil for low Reynolds number applications, based on the data shown in Figures 3-1 and 3-2.

Below a Reynolds number of approximately 1.0×10^6, there is not anything to be gained, insofar as the minimum drag coefficient is concerned, by using aerofoils of the NACA 6-series. Older aerofoils such as the NACA 4412 or the NACA 4415 are preferable to laminar flow aerofoils of the same thickness. Figure 16-a of Loftin and Smith's report, reproduced here as Figures 3-3 and 3-4 shows that the trend of the minimum drag coefficient for all of the laminar flow sections tested is towards an accelerating increase as the Reynolds number falls below 2×10^6.

The two NACA 5-digit aerofoils tested exhibit the same trend, though clearly not to the same extent as the laminar flow sections. The minimum drag coefficient of the three NACA 4-digit aerofoils are also increasing but at a more-or-less constant rate. Projecting, in the mind, the curves to Reynolds numbers below 0.7×10^6, one can visualize the lower section drag coefficients of the older aerofoils. Of course this conjecture should be verified experimentally.

When the highest possible lift coefficients are desired below $Re = 1.0 \times 10^6$, the laminar flow aerofoils are at even more of a disadvantage than they are with respect to the minimum section drag coefficients. Of all the aerofoils tested by Loftin and Smith, those that pass the projection test with the highest marks are the NACA 4412 and the NACA 4415.

The aerofoil with the lowest drag at Re = 0.7×10^6 is, as shown in Figure 3-3, the NACA 64-409. However, the maximum lift coefficient for this aerofoil at the same Reynolds number is 1.08, considerably lower than that of the NACA 4-digit sections.

The 11.7% thick Clark Y has both a higher drag coefficient and a lower lift coefficient than either of the NACA 4-digit sections.

Curves of $(C_L/C_D)_{max}$ versus Reynolds number were plotted using the data of references [14] and [15] for several conventional aerofoils and are shown in Figure 3-5. The maximum C_L/C_D can be taken as a measure of the efficiency of an aerofoil and also as an indication of its tolerance to off design operation since maximum C_L/C_D will always occur at a lift coefficient somewhat higher than design C_L.

The NACA 4-digit series aerofoils are again better than the laminar sections at low Reynolds numbers.

While the older aerofoils, such as the NACA 4412 have been shown to be better at low Reynolds numbers than the newer NACA 6-series sections, the situation is reversed at the higher Reynolds numbers. The investigation into the effects of surface roughness carried out in reference [15], although very narrow in scope, showed that surface roughness tends to equalize the performance of the two classes of aerofoils at high Reynolds numbers.

3.3 Preliminary Results

The best conventional aerofoil for low Reynolds number applications can now be chosen. The NACA 4412 and the NACA 4415 were the best of all those considered. Of these two, the NACA 4412 is the

better. How these aerofoils compare with those specially designed for low Reynolds number will be seen in the next chapter.

CHAPTER IV

LOW REYNOLDS NUMBER AEROFOILS

As was the case with conventional aerofoils, experimental data at low Reynolds numbers on aerofoils specifically designed for low Reynolds numbers is scarce. In fact, aerofoils specifically designed for low Reynolds numbers are themselves scarce.

Low Reynolds number aerofoils have been designed by R. Eppler [16] and F.X. Wortmann [17], [18], [13]. A few experimental investigations have been conducted on these aerofoils, though these are not as comprehensive as the investigation of reference [15]. Some NACA sections have been designed for helicopter applications [19] and these qualify as low Reynolds number aerofoils. A few special aerofoils have been developed for man powered aircraft [1], [20] but no experimental data was found. Dolphin fin profiles have even been proposed as having possible applications [21], although no one has tried them yet.

Measurements made on most of the low Reynolds number aerofoils did not systematically investigate the effect of parameters such as thickness to chord ratio, as was done in reference [15].

But this is almost to be expected. The aerofoils examined in reference [15] had been in existence for years before the investigation was done. Almost all the aerofoils belonged to one family that changed in a regular and continuous manner. The investigation covered a relatively large number of aerofoils, all tested in the same tunnel. This means that the findings on one aerofoil can be directly compared

with those of another.

This is not the case where low Reynolds number aerofoils are concerned. These aerofoils have been developed in several small groups. The members of each group are significantly different than the members of the other groups, and sometimes are different within a group. The experimental investigations have usually been carried out shortly after the design of the aerofoils and only on the aerofoils presented in the design. Several wind tunnels have been employed in the tests and, probably, different methods used for making the measurements and reducing the data. All this means that comparison of different low Reynolds number aerofoils is both more difficult and less meaningful than for conventional aerofoils.

Curves of the aerodynamic characteristics, maximum lift coefficient and minimum drag coefficient, for low Reynolds number aerofoils appear in Figures 4-1 and 4-2. The lift-drag ratio for these aerofoils is presented in Figures 4-3, 4-4, 4-5 and 4-6. All of the aerofoils for which experimental data is available are represented. Also presented in the figures are data for some NACA 6-series aerofoils that were tested with the low Reynolds number aerofoils for purposes of comparison. The data for the aerofoils came from the following sources.

Reference [13]	FX 60-126
	FX 61-140
	FX 61-163
	FX 61-184

Reference [18]	FX 2
	FX 05-191
	FX 05-188
	FX 08-S-176
	FX 05-H-126
	NACA 8-H-12
	NACA 64-418
Reference [19]	NACA 11-H-09
	NACA 12-H-12
	NACA 13-H-12
	NACA 14-H-12
	NACA 15-H-15
	NACA 8-H-12
Reference [22]	FX 1057-816
	NACA 65-714
Reference [23]	EC 86(-3)-914

4.1 Designs due to Eppler

R. Eppler [16] has developed what he calls "a novel idea" for the computation of laminar aerofoil sections, with emphasis on the Reynolds number range of gliders. He takes a different approach to the design of low drag aerofoil sections from that of the NACA 6-series in that the aerofoils are intended to have laminar boundary layers on one side only, with an optimized turbulent boundary layer on the suction side.

His aerofoil designation is based on the NACA system of numbering.

Consider the designation EB 8(-1)-012. The "8" designates laminar regions up to x/c = 0.8. The "-1" indicates a gap of twice 0.1 between the lift coefficients of the two laminar effects. The "012" means the same as in the NACA numbering; design lift = 0 and 12% thickness.

Although Eppler's aerofoils have been used on a number of sailplanes, they do not appear to have been widely accepted. This is probably at least partly due to a lack of experimental data on their performance. Only one report was found which gave any experimental information. This investigation [23] was a particularly interesting one in that it obtained data on boundary layer development and also in that it was carried out in free flight giving the best possible simulation of service conditions.

4.1.1 Theoretical Considerations

Eppler's aerofoils were designed to have longer laminar stretches on the pressure side of the aerofoil and a reduced adverse pressure gradient on the suction side. The lessening of the adverse pressure gradient is to reduce the danger of separation of the turbulent boundary layer. A large nose radius is used to favourably influence the maximum lift coefficient. The difference between Eppler's pressure distribution and that of a NACA 6-series section may be seen in Figure 4-7.

For a symmetrical Eppler aerofoil section at $C_L = 0$, a suction peak exists near the nose on both the upper and lower sides and the aerofoil has a turbulent boundary layer over almost its entire surface. The NACA 6-series aerofoil, for the same case, has the suction

peak well back along the chord, and has laminar flow on both sides back to approximately this point.

The Eppler section is so designed that for a small positive angle of attack, for example 0.9° corresponding to a lift coefficient of 0.1, the suction peak on the lower surface disappears and is replaced by either constant pressure or by a favourable pressure gradient over the forward part of the aerofoil. This results in a laminar flow on the lower surface back to approximately $x/c = 0.6$. After this point, the pressure gradient becomes unfavourable. For the rear part of the aerofoil, instead of using a constant positive pressure gradient similar to that of the NACA 6-series sections, a pressure gradient is used that resembles those suggested by F.X. Wortmann [17]. Such a pressure gradient reduces the danger of turbulent separation towards the trailing edge of the lower surface.

The suction peak on the upper surface is intensified near the nose but, because of the relatively thick nose radius, the additional suction peak is small. This pressure increase on the upper surface is found largely near the nose, so that the adverse pressure gradient near the nose is markedly increased while there is only a slight increase over the portion just preceeding the mid-chord position. By locating the transition point before the start of the pressure rise, the turbulent boundary layer will have a small enough thickness to resist separation through the strong adverse pressure gradient which immediately follows the suction peak. Thereafter, the adverse pressure gradient is significantly weaker and may not induce separation until some point relatively far back on the aerofoil chord.

For the NACA 6-series section, a corresponding small positive angle of attack intensifies the already favourable pressure gradient on the lower surface. However, the suction peak remains in the same position and transition in the flow from laminar to turbulent still takes place here. When the lift coefficient exceeds a value of approximately $C_L = 0.12$, the upper suction peak on the NACA 64_1-012 moves to a position near the nose. The suction peak at the nose will rapidly increase in intensity with increasing angle of attack, and if the Reynolds number is low the laminar boundary layer may separate in the strong adverse pressure gradient following the peak. This effect is accentuated if the aerofoil has a small radius leading edge.

The NACA 4-digit aerofoils avoid laminar separations of this kind because the suction peak at the nose tends to be of the right shape to cause transition rather than laminar separation. This would account for their better low Reynolds number performance. Similarly, the Eppler aerofoils have a relatively large nose radius to avoid laminar separations at high C_L.

The polar diagrams of the new aerofoils are expected to be as shown in Figure 4-8. The laminar effects, which do not overlap as they do for NACA 6-series sections, are considerably stronger than the laminar effects of the NACA 6-series sections [16]. One of the laminar effects can be made to extend beyond lift coefficients of unity by using a positive camber which would simply displace the whole curve to the right.

4.1.2 Experimental Results

The only available experimental data on an Eppler aerofoil is contained in an examination conducted by A. Raspet and D. Györgyfalvy [23]. The tests consisted of both free flight and wind tunnel measurements. The aerofoil examined was the EC 86(-3)-914 and the investigation showed that it has excellent performance. The experimental drag polar shown in Figure 4-9 shows the two low drag regions predicted by Eppler. A flight test of this aerofoil mounted on a Pheonix sailplane, showed that at a Reynolds number of 0.9×10^6, the maximum lift coefficient was a very high 1.75.

The upper surface, for chord positions x/c greater than approximately 0.6, experienced laminar separation at low lift coefficients and turbulent separation at high lift coefficients. At low lift coefficients, the lower surface experienced relatively early transition and turbulent separation towards the trailing edge. The boundary layer development on the upper and lower surfaces is shown in Figure 4-10.

The available experimental data concerning the EC 86(-3)-914 has been plotted in Figure 4-2(a).

4.2 Designs due to Wortmann

Another series of aerofoils especially intended for low Reynolds number applications have been designed by F.X. Wortmann [17], [18], [13].

The philosophy behind Wortmann's aerofoils is basically the same as that of the NACA 6-series laminar flow sections, except that the control of the boundary layer is given a more detailed treatment.

The pressure gradient over the rear part of the aerofoil is designed to obtain minimum drag from the turbulent portion of the boundary layer. An instability region is introduced to make sure that transition from laminar to turbulent flow takes place at the desired place on the aerofoil surface. Some thought is given to design of the nose shape of the aerofoil to avoid laminar separation at high C_L.

No general explanation covering all of Wortmann's aerofoil designations can be offered except for mentioning that the figures following the hyphen indicate the aerofoil thickness as a percentage of the chord.

4.2.1 Theoretical Considerations

In Wortmann's first report [17], his alteration of the back part of the pressure distribution was relatively simple. The optimum solution was regarded to be one which would keep the turbulent boundary layer just on the verge of separation. The required pressure distribution results in a relatively large initial pressure gradient, decreasing toward the trailing edge. The optimum velocity distribution is assumed to be one which results in a constant value of 1.8 for the form parameter in the turbulent region. This velocity distribution would result in the steepest possible non-separating pressure distribution at the tail of the aerofoil and the longest possible laminar boundary layer. Therefore the longest permissible favourable pressure gradient can be determined, resulting in laminar flows over greater portions of the upper surface than had hitherto been achieved. A reduction in drag is the expected result.

Such a distribution takes into consideration the ability of the turbulent boundary layer to drive against an adverse pressure gradient. This distribution also pits the turbulent boundary layer at its thinnest against the steepest adverse pressure gradient. As the turbulent boundary layer becomes thicker further along the chord, it meets adverse pressure gradients that become weaker. A sketch of the required velocity distribution is compared with the type used on the NACA 6-series sections in Figure 4-11.

The results of a test on an aerofoil designed in connection with reference [17] indicated that the performance was not as good as had been expected. The unexpectedly poor performance was caused by the transition point not being in the expected location. It was supposed to be located at the beginning of the pressure rise region, but instead it was found some distance downstream. It even passed beyond the theoretically computed position of laminar separation.

In a subsequent report [18], Wortmann discusses the problems associated with the aerofoils of reference [17] and presents a slightly modified approach to the design of low Reynolds number aerofoils.

The pressure distributions used for the aerofoils in the latter report are still largely based on the work done in reference [17]. However, a region of either constant pressure or slightly increasing pressure is introduced between the regions of pressure drop and the rapid pressure rise. This region is called the instability region and its purpose is to ensure that the laminar boundary layer experiences transition to turbulence before the rapid pressure rise is encountered.

After the boundary layer has become turbulent, it may enter the region of rapid pressure rise without fear of immediate separation.

Wortmann has also given some attention to the aerofoil nose shape and has shown [24] that improvement in performance at high lift coefficients can be made.

The aerofoil shape near the leading edge can be designed to reduce the intensity of the suction peak occurring there at high lift, and thus avoid problems with laminar separations. Wortmann was able to improve the high lift performance of an existing aerofoil, the NACA 63-618, by small modifications to the leading edge shape. A wider low drag region and higher maximum lift coefficient were obtained.

4.2.2 Experimental Results

Data on Wortmann's aerofoils are given in references [22], [18], and [13]. The results of these three investigations are discussed in chronological order. The particular aerofoils discussed under each subheading below are noted on pages 26 and 27.

Reference [22]

Some experimental data comparing the FX 1057-816 with the NACA $65_{(215)}$-714 are given in reference [22]. The FX 1057-816 was designed following the theory of reference [17], which does not provide an instability region to regulate the position of transition. Reference [17] presented a method whereby the optimum pressure distribution could be determined, resulting in an aerofoil with longer laminar boundary layers compared to the NACA 6-series sections.

Data on the two aerofoils of reference [22] is shown in

Figure 4-1(a). The drag coefficients of the two aerofoils were found to be quite similar. The lift coefficients of both aerofoils vary irregularly with Reynolds number in that they do not steadily increase with increasing Reynolds number. The author of reference [22] mentions that the lift measurements taken could not be corrected for end effects so perhaps the lift coefficient data should be ignored.

The position of transition for the two aerofoils was determined at various lift coefficients for the three Reynolds numbers covered in the investigation. The location of the transition point versus lift coefficient and the lift-drag polar are shown in Figure 4-12. At the lower Reynolds numbers the laminar trough of the FX 1057-816 is considerably wider than that of the NACA $65_{(215)}$-714. Note how the width of the laminar troughs are related to the position of transition. Figure 4-12 indicates that the goal of reference [17] was achieved in that longer laminar stretches over the aerofoil have been realized.

The maximum thickness of the NACA aerofoil is 14% of the chord length while that of the FX section is 16%. Based on the results of reference [15], increasing the maximum thickness of the NACA aerofoil to 16% would have resulted in approximately 9% greater profile drag than for the FX aerofoil.

It should be mentioned that some difficulties were encountered in the experimental investigation. The pressure taps on the NACA section were defective and resulted in a less accurate determination of the pressure distribution for this profile than for the FX section. How this would influence the results is not known but at least the data

for the FX section can be considered accurate.

The data of reference [22] was used to plot curves of $(C_L/C_D)_{max}$ versus Reynolds number. The curves for the two aerofoils of reference [22] appear in Figure 4-3.

Reference [18]

Another group of aerofoils were built and tested by Wortmann. These aerofoils are based on the theory of reference [18] and all but one, the FX 2, have been designed with an instability region. Six new low Reynolds number aerofoils were tested and these were compared against two NACA aerofoils.

Both the NACA aerofoils had previously been tested below $Re = 2 \times 10^6$ and, therefore, could be used as a guide in comparing the performance of the wind tunnel used in reference [18] with the NACA tunnel. The results of the test show that, in the region of the laminar trough, the drag coefficient is virtually the same for the two tunnels. The width of the laminar trough, as measured in the tunnel of reference [18], was approximately 20% below the value measured in the NACA tunnel. This was true for both profiles. The maximum lift coefficient measured was likewise found to be 10-25% too low.

The six newly designed and tested aerofoils of reference [18] are intended specifically for the Reynolds number range of 0.5×10^6 to 3.0×10^6. The available experimental data for four of the new sections is shown in Figure 4-1(b). Data for a fifth section, the FX 2, appears in Figure 4-1(a).

The results of the tests show that the ideas that appear in references [17] and [18] do result in considerable improvement in aero-

foil performance. For example, Figure 4-13 shows that two new sections, both with approximately 19% thickness, have about 18% lower drag than a comparable 18% thick NACA 6-series section. When these two new sections are compared with a 12% thick NACA laminar flow aerofoil, the NACA 8-H-12, the minimum drag coefficients are very nearly the same but the width of the laminar trough of the new sections is considerably greater. Figure 4-1(b) shows that these improvements are not gained by sacrificing a high maximum lift coefficient.

Curves of $(C_L/C_D)_{max}$ versus Reynolds number for the aerofoils of reference [18] are shown in Figure 4-4, except for the FX 2 which appears in Figure 4-3.

Reference [13]

Four more aerofoil sections specifically designed for sail planes appear in reference [13]. These aerofoils are, again, designed on the basis of theory presented in references [17] and [18]. They show significant reductions in the profile drag coefficient.

The available experimental data of reference [13] is shown in Figure 4-2(a). The data of reference [13] was used to plot curves of $(C_L/C_D)_{max}$ versus Reynolds number and these curves are presented in Figure 4-5.

4.3 NACA Helicopter Aerofoils

Several aerofoils have been designed by NACA for helicopter applications. An experimental investigation of five of these sections is presented in a report by Schaefer et al [19]. These aerofoils were developed a few years after the introduction of the laminar flow aero-

foils and were designed to take advantage of the low profile drag coefficients associated with the attainment of relatively large extents of laminar flow. The five sections presented in reference [19] use the basic thickness form of the NACA 64 series. They are different from the conventional aerofoils in that the aerofoil camber lines have been altered to yield the nearly zero pitching moments that are of prime importance in helicopters.

Experimental measurements were taken at Reynolds numbers of 0.9×10^6, 2.0×10^6 and 2.6×10^6. The maximum lift coefficients, and the minimum drag coefficients for the five sections are plotted against Reynolds number in Figure 4-2(b). The maximum lift drag ratio is plotted against Reynolds number in Figure 4-6. Reference [19] also presents data for the NACA 8-H-12 which is taken from an earlier NACA publication, NACA RB L5K02(1946). The NACA 8-H-12 was judged to be the best section of the four sections tested in that paper. In reference [19], the NACA 11-H-09 was chosen as the best of the five sections tested and was said to be approximately equal in performance to the NACA 8-H-12.

4.4 Other Low Reynolds Number Aerofoils

4.4.1 Aerofoils for Man Powered Aircraft

Other aerofoils have been designed for low Reynolds number applications but as mentioned before, no data can be found concerning them. Aircraft designed for man powered flight require low Reynolds number aerofoils and remarks concerning two different aerofoils for this application appear in the literature. One is the Wortmann FX-63137,

which is specifically intended for use in a man powered aircraft [1]. The Reynolds number for which it was designed is approximately 0.6×10^6. An aerofoil with the basic thickness form NACA 0012 and a mean line a = 0.3 has been selected by a Canadian group for use in a man powered aircraft [20]. The results of some wind tunnel tests on this aerofoil were mentioned. At a Reynolds number of 0.9×10^6, the maximum lift coefficient was 1.65 and the minimum profile drag measured was 0.011 at a lift coefficient of 1.0. At minimum drag, laminar flow extends over the first 35% of the upper surface and the first 85% of the lower surface.

If the two above mentioned cases can be taken as general examples, then it seems that, as mentioned earlier, the development of low Reynolds number aerofoils is going to be quite irregular. The aerofoils will not be well catalogued and experimental data is going to be hard to obtain and difficult to use for comparisons.

4.4.2 Designs Based on Nature

Man is still trying to copy the flight of living things in his search for better and better flying machines. This time, however, it is not the flight of birds through the air that is being examined, but rather, the flight of dolphins through the sea.

T.G. Lang [21] suggests dolphin fins as a possible model on which to base the design of low Reynolds number aerofoils. Profiles of two dorsal fins and one tail fluke were plotted graphically and a smooth curve was run through the plotted points. These curves were then used to calculate the pressure distributions of the three profiles. The profile and the pressure distribution of one fin are shown in

Figure 4-14.

The fins all have similar physical characteristics. The maximum thicknesses are all located between 32 and 36 percent of the chord length and the ratio of thickness to chord length ranges from 15 to 21 percent. The pressure minimums are located between 14 and 16 percent of the chord length, and they all have a fairly long region of gentle adverse pressure gradient followed by a steep adverse pressure gradient towards the trailing edge.

Lang says that an analysis of the fin pressure distributions indicates that these fin sections are ideally suited for use at their usual service Reynolds numbers of around 10^6. He suggests that these dolphin fins are a compromise between aerofoils designed by Wortmann and Eppler, the FX 05-191 and the EA 6(-1)-018 respectively. The differences between these two aerofoils are so great that a compromise design might have many unexpected beneficial characteristics [21].

4.5 Results

A survey of the collected data shows that no one group of aerofoils has the best performance in all fields. The highest maximum lift coefficients belong to aerofoils of references [23] and [13]. The lowest minimum drag coefficients are those of the aerofoils in reference [19] and the best $(C_L/C_D)_{max}$ characteristics can be associated with the aerofoils of reference [18].

Only one fact is clearly obvious. The aerodynamic characteristics of conventional aerofoils are not nearly as good at low Reynolds numbers as those of low Reynolds number aerofoils. The best of the conventional

aerofoils, according to Section 3.3, were the NACA 4412 followed closely by the NACA 4415. Comparing the maximum lift coefficient and the minimum drag coefficient of these two aerofoils with those of the FX 60-126 or the FX 61-163, for example, shows that the FX 60-126 is definitely superior in both aspects while the FX 61-163 has better drag characteristics and approximately equal lift characteristics.

The aerofoils with the best maximum lift coefficient at low Reynolds numbers are the EC 86(-3)-914, the FX 60-126, the FX 61-140 and the FX 61-163. All these aerofoils appear in Figure 4-2(a). These same four aerofoils, with the exception of two helicopter sections, also have the lowest minimum drag coefficients. The two helicopter sections that have lower minimum drag coefficients are the NACA 11-H-09 and the NACA 12-H-12. No data could be found for NACA tests on the NACA 8-H-12 below a Reynolds number of 2×10^6. Above this number it has good drag characteristics. While the NACA 11-H-09 and the NACA 12-H-12 have only slightly lower minimum drag coefficients than the 4 previously mentioned sections, their maximum lift coefficients are considerably lower. Two helicopter sections approach the maximum lift coefficients of the FX 61-140 and the FX 61-163. These are the NACA 14-H-12 and the NACA 15-H-15. Their minimum drag coefficient, however, are significantly higher.

Therefore considering the maximum lift coefficients and the minimum drag coefficient, the best low Reynolds number aerofoils are the EC 86(-3)-914, the FX 60-126 and the FX 61-163.

From the plots of $(C_L/C_D)_{max}$ versus Reynolds number, the

best aerofoils are those of reference [18], particularly above Reynolds numbers of 1.0×10^6. The best aerofoil of all is the FX 05-H-126. As the Reynolds number falls below 0.8×10^6, the curves of $(C_L/C_D)_{max}$ versus Reynolds number for the aerofoils of reference [18] approach the curves for the aerofoils FX 61-163 and the FX 60-126. The aerofoils of reference [18] appear to have faster falling curves. Projecting, in the mind, the curves to slightly beyond $Re = 0.7 \times 10^6$, it is highly probable that the curves of $(C_L/C_D)_{max}$ versus Reynolds number for the aerofoils FX 61-163 and FX 60-126 would be approximately equal to or just slightly lower than those of the reference [18] aerofoils.

It is unfortunate that more extensive tests were not performed upon some of Eppler's aerofoils. The single points plotted in Figure 4-2(a) indicate that the EC 86(-3)-914 has the highest maximum lift coefficient of all the specially designed low Reynolds number aerofoils. Its minimum drag coefficient is lower than all but the two helicopter sections, the NACA 11-H-09 and the NACA 12-H-12. The only category in which this aerofoil does not compare favourably is $(C_L/C_D)_{max}$. At $Re = 1.2 \times 10^6$ it is approximately 10% lower than the curve for the FX 61-163 and 5% lower than the curve for the FX 60-126.

There is some evidence that the results for the low Reynolds number aerofoils designed by Wortmann and Eppler would have been even better if they had been tested in the NACA low turbulence tunnel. Higher turbulence levels in the wind tunnels used for tests on the new aerofoil sections gave a narrower drag bucket and lower maximum lift for the NACA laminar flow sections tested in reference [18]. This was previously noted in section 4.2.2.

CHAPTER V

CONCLUSIONS AND RECOMMENDATIONS

5.1 The Best Aerofoil or Group of Aerofoils

The best group of aerofoils for which test data could be found consists of the FX 60-126, the FX 61-163 and the EC 86(-3)-914. These three aerofoils have the highest maximum lift coefficients and come close to having the lowest minimum drag coefficients at low Reynolds numbers.

5.2 Recommendations for Further Study

An investigation, similar to that of reference [15], should be carried out for some of the more recent low Reynolds number aerofoils. Some of Eppler's aerofoils should certainly be investigated. Perhaps the Reynolds number range could be extended down to approximately 0.2×10^6 for the aerofoils tested.

There seems to be sufficient data available on the NACA 6-series sections for Reynolds numbers down to 0.7×10^6. Some low Reynolds number data for NACA 4-digit and 5-digit sections appears in reference [25]. Comparing this data with that of reference [15], it is seen that the maximum lift coefficients of the same aerofoils in the two studies are approximately equal but the minimum drag coefficients of reference [24] are higher than those measured in reference [15]. Based on the data of reference [25], the NACA 4409 would probably

prove to have low Reynolds number characteristics competitive with low Reynolds number aerofoils.

Any further tests should, if possible, be of a large number of aerofoils, all tested in one wind tunnel rather than in many different tunnels by different groups of investigators. This would make the results all the more valuable in that no accounting would have to be made for differences in turbulence levels in the various wind tunnels.

Perhaps the methods used in the design of low Reynolds number aerofoils could be put to good use at higher Reynolds numbers. The turbulent boundary layer might benefit from being confronted with a steadily decreasing adverse pressure gradient rather than the type used on the NACA 6-series aerofoils.

The effect of surface roughness on the aerodynamic characteristics of low Reynolds number aerofoils has not been investigated, and has been only crudely investigated for standard aerofoils. The roughness test of reference [15] consisted of placing a coating of carborundum grains over a portion of the aerofoil nose. There was no variation in the grain size, density of coating, or the extent of the coating. The crude roughness tests performed changed the aerofoil characteristics radically and showed that there is little difference between severely roughened aerofoils, no matter what the original section is. A more interesting investigation would determine the largest irregularities in construction or paint work that can be tolerated without losing the original characteristics. Some sections may prove more tolerant than

others. The Eppler sections especially might perform well with roughened surfaces since the design method stipulates that the upper surface is to experience early transition to turbulence. All the other aerofoils depend upon long laminar stretches over the upper surface for their good characteristics. These laminar stretches might tolerate less roughness than Eppler's turbulent boundary layer before the deterioration of the aerodynamic characteristics begins.

LIST OF REFERENCES

[1] Shenstone, B.S. - Unconventional Flight, J. Roy. Aero. Soc., Vol. 72, 655-666, 1968.

[2] Schlichting, H. - Boundary Layer Theory, Sixth Edition, McGraw-Hill Inc., New York, 1968.

[3] Bradshaw, P. and Pankhurst, R.C. - The Design of Low-speed Wind Tunnels, contribution to Progress in the Aeronautical Sciences, (Editor-D. Küchemann), Pergamon Press, Vol. 5, 2-69, 1964.

[4] Dryden, H.L. - Transition from Laminar to Turbulent Flow, contribution to High Speed Aerodynamics and Jet Propulsion, (Editor-C.C. Lin), Princeton University Press, Vol. 5, 3-75, 1959.

[5] Gault, D.E. - An Experimental Investigation of Regions of Separated Laminar Flow, NACA TN 3505, 1955.

[6] Kuethe, A.M. and Schetzer, J.D. - Foundations of Aerodynamics, Second Edition, John Wiley and Sons, Inc., New York, 1967.

[7] Schubauer, G.B. and Skramstad, H.K. - Laminar Boundary-Layer Oscillations and Stability of Laminar Flow, J. Aero. Sci., Vol. 14, 69-78, Feb., 1947.

[8] Tani, I. - Low-Speed Flows Involving Bubble Separations, contribution to Progress in the Aeronautical Sciences, (Editor-D. Küchemann),Pergamon Press, Vol. 5, 70-103, 1964.

[9] Dryden, H.L. - Review of Published Data on the Effect of Roughness on Transition from Laminar to Turbulent Flow, J. Aero. Sci., Vol. 20, 477-482, July, 1953.

[10] Riegels, F.W. - Aerofoil Sections, Butterworth and Co. Ltd., London, 1961.

[11] Smith, A.M.O. and Clutter, D.W. - The Smallest Height of Roughness Capable of Affecting Boundary-Layer Transition, J. Aero/Space Sci., Vol. 26, 229-245, April, 1959.

[12] Smith, A.M.O. and Kaups, K. - Aerodynamics of Surface Roughness and Imperfections, S.A.E. Publication #680198, April, 1968.

[13] Wortmann, F.X. - Some Laminar Profiles for Sailplanes, Soaring, 14-18, January, 1964.

[14] Silverstein, A. - Scale Effect on Clark Y Airfoil Characteristics from NACA Full-Scale Wind Tunnel Tests, NACA TR 502, 1934.

[15] Loftin, Jr., L.K. and Smith, H.A. - Aerodynamic Characteristics of 15 NACA Airfoil Sections at Seven Reynolds Numbers from 0.7×10^6 to 9.0×10^6, NACA TN 1945, 1949.

[16] Eppler, R. - Laminarprofile für Segelflugzeuge, Z.F.W., Vol. 3, (10), 345-353, 1955. (British M.O.A. Translation TIL/T. 4904, 1960).

[17] Wortmann, F.X. - Ein Beitrag zum Entwurf von Laminarprofilen für Segelflugzeuge und Hubschrauber, Z.F.W., Vol. 3, (10), 333-345, 1955. (British M.O.A. Translation TIL/T. 4903, 1960).

[18] Wortmann, F.X. - Experimentelle Untersuchungen an Neuen Laminarprofilen für Segelflugzeuge und Hubschrauber, Z.F.W., Vol. 5, (8), 228-243, 1957. (British M.O.A. Translation TIL/T. 4906, 1960).

[19] Schaefer, R.K., Loftin, Jr., L.K. and Horton, E.A. - Two Dimensional Investigation of Five Related NACA Airfoil Sections Designed for Rotating-Wing Aircraft, NACA TN 1922, 1949.

[20] Czerwinski, W. - Structural Trends in the Development of Man-powered Aircraft, J. Roy. Aero. Soc., Vol. 71, 9-13, 1967.

[21] Lang, T.G. - Hydrodynamic Analysis of Dolphin Fin Profiles, Nature, Vol. 209, 1110-1111, 1966.

[22] Speidel, L. - Messungen and Zwei Laminarprofilen für Segelflugzeuge, Z.F.W., Vol. 3, 10, 353-359, 1955. (British M.O.A. Translation TIL/T. 4905, 1960).

[23] Raspet, A. and Györgyfalvy, D. - Boundary Layer Studies on the Pheonix Sailplane, OSTIV Publication VI, 1960.

[24] Wortmann, F.X. and Althaus, D. - Messungen an drei Flügelprofilen des Segelflugzeuges Ka 6, OSTIV Publication Vi, 1960.

[25] Jacobs, E.N. and Sherman, A. - Airfoil Section Characteristics as Affected by Variations of the Reynolds Number, NACA TR 586, 1937.

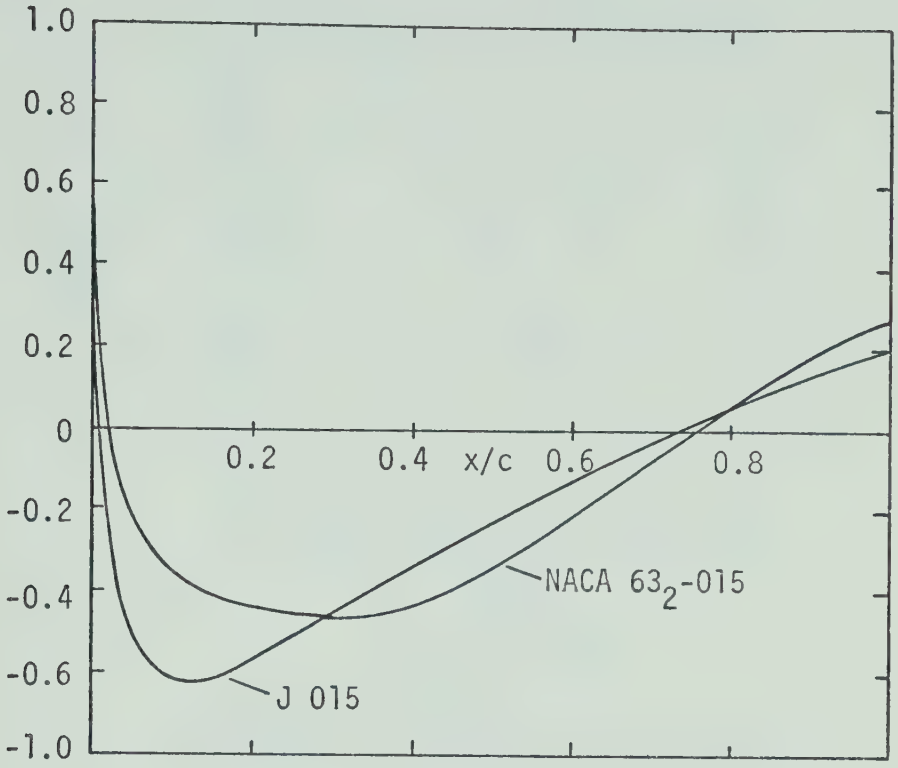

FIGURE 2-1[10]

PRESSURE DISTRIBUTIONS ON TWO AEROFOILS AT $C_L = 0$

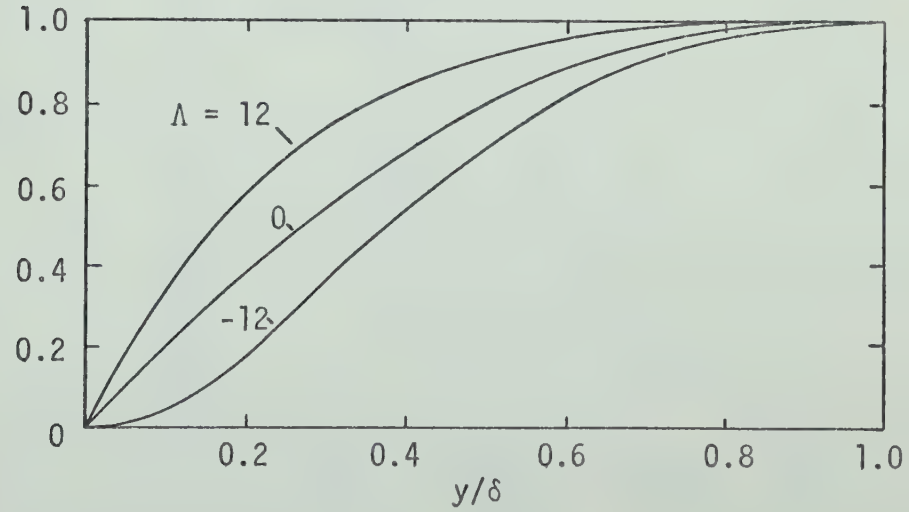

FIGURE 2-2[2]

VARIATION OF VELOCITY PROFILES WITH SHAPE FUNCTION Λ

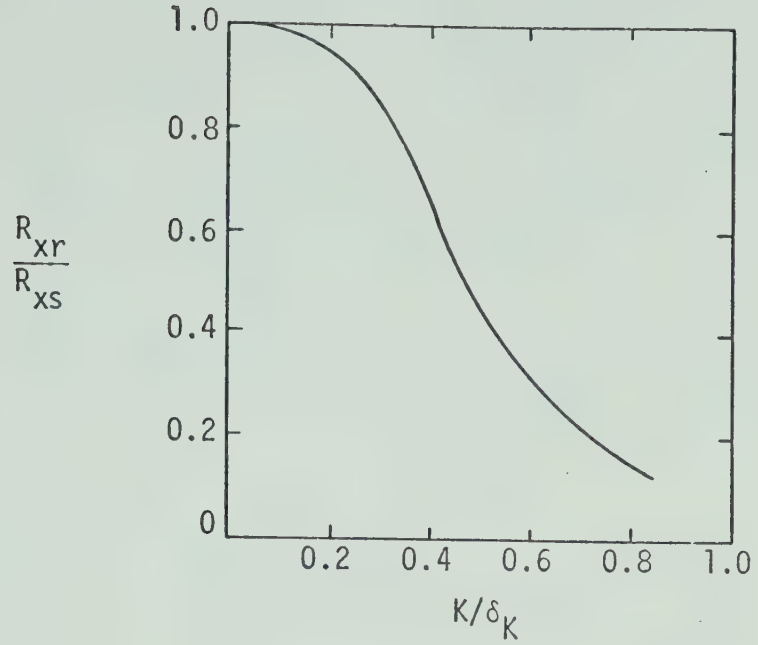

FIGURE 2-3[9]

INFLUENCE OF ROUGHNESS ON TRANSITION

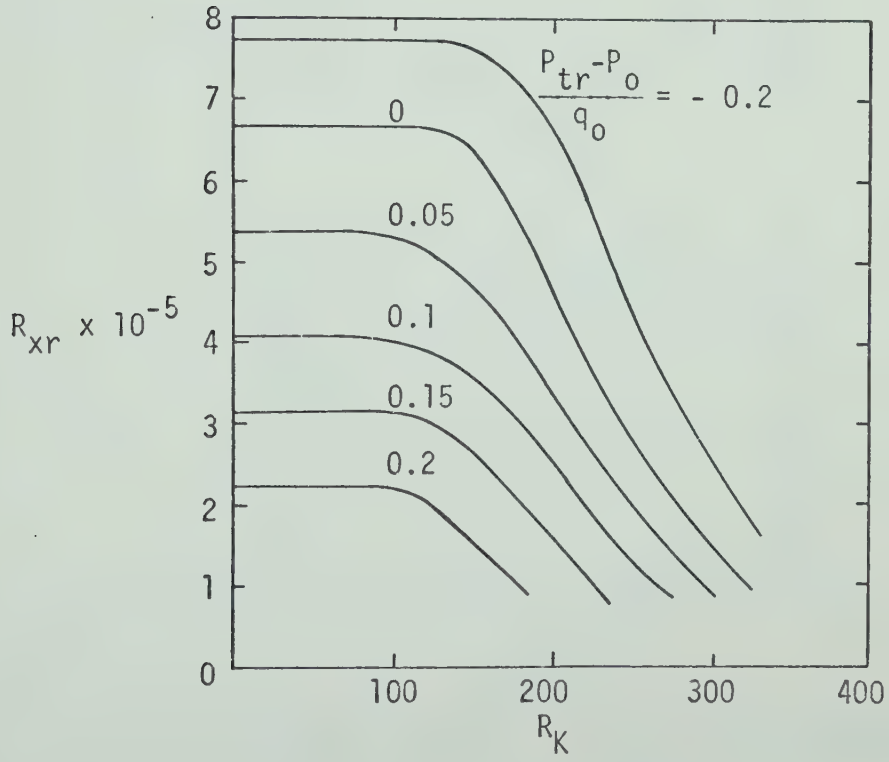

FIGURE 2-4[2]

INFLUENCE OF PRESSURE GRADIENT AND ROUGHNESS ON TRANSITION

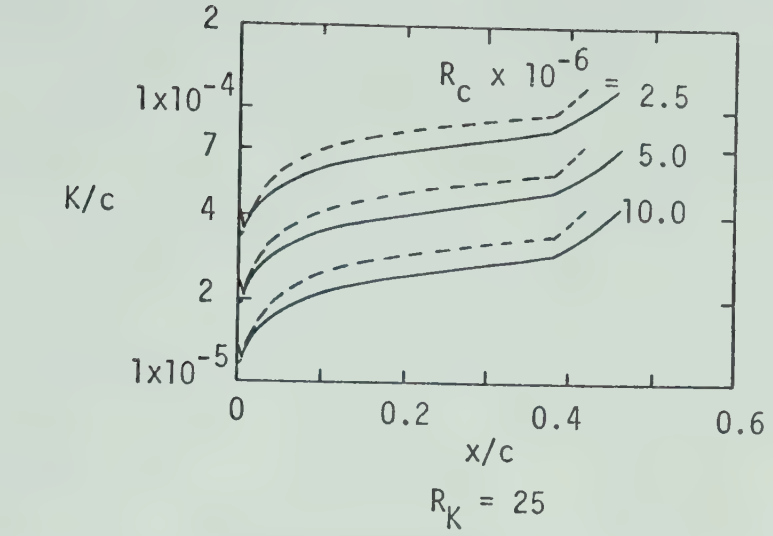

R_K = 25

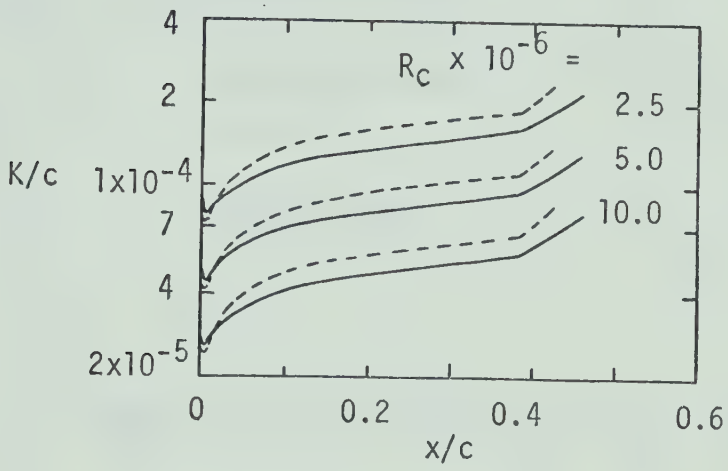

R_K = 100

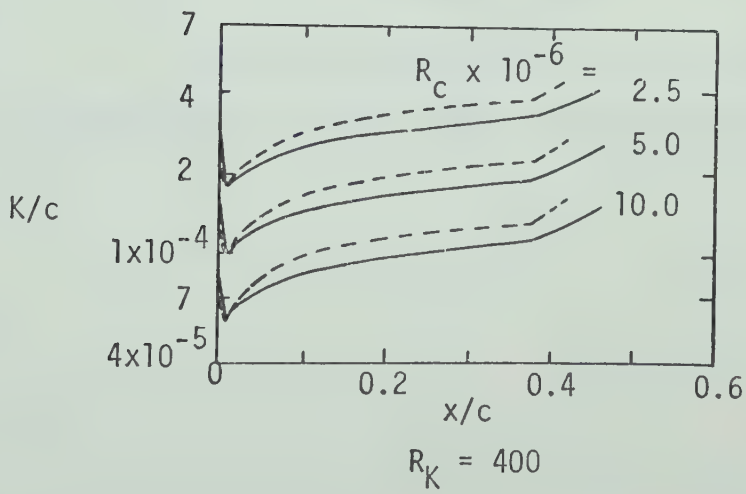

R_K = 400

——— upper surface, — — — lower surface

FIGURE 2-5[12]

ALLOWABLE ROUGHNESS HEIGHT ON NACA 64-415 AT C_L = 0.4

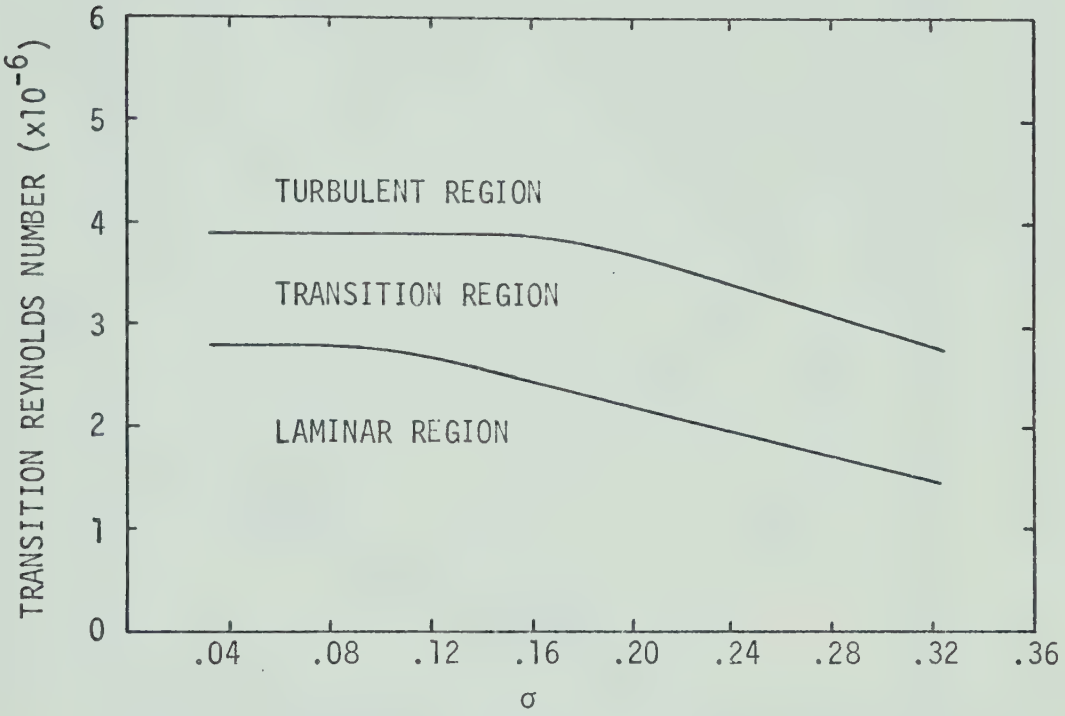

FIGURE 2-6[7]

EFFECT OF TURBULENCE ON REYNOLDS NUMBER OF TRANSITION FOR A FLAT PLATE WITH ZERO PRESSURE GRADIENT

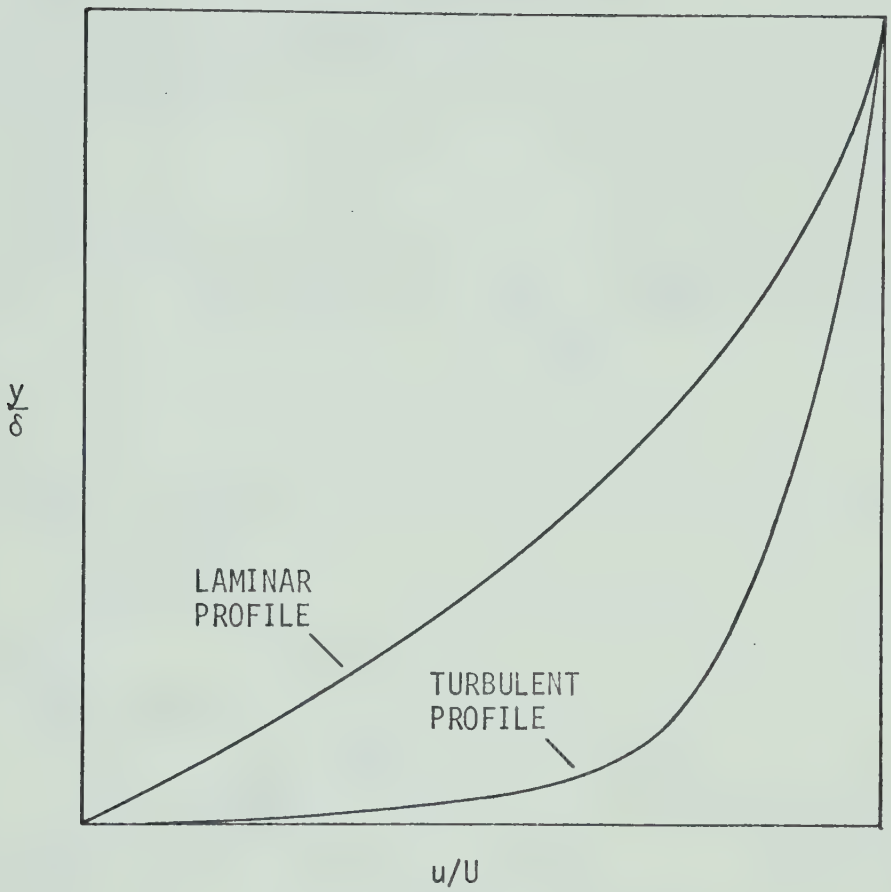

FIGURE 2-7[6]

COMPARISON BETWEEN LAMINAR AND TURBULENT VELOCITY PROFILES

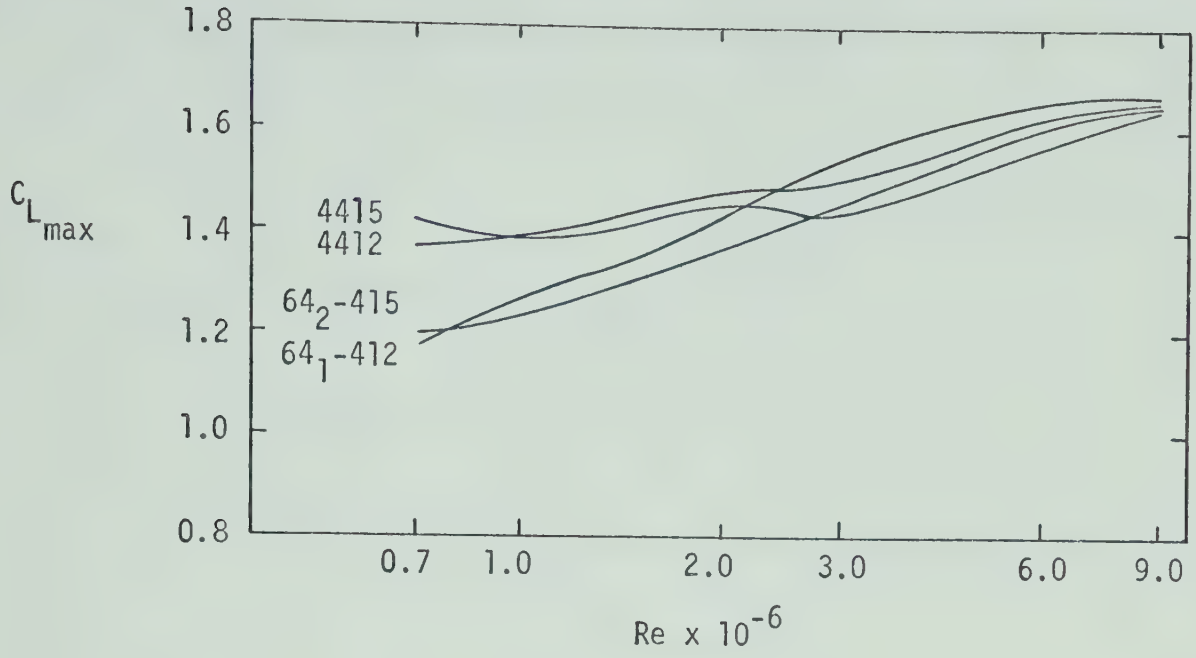

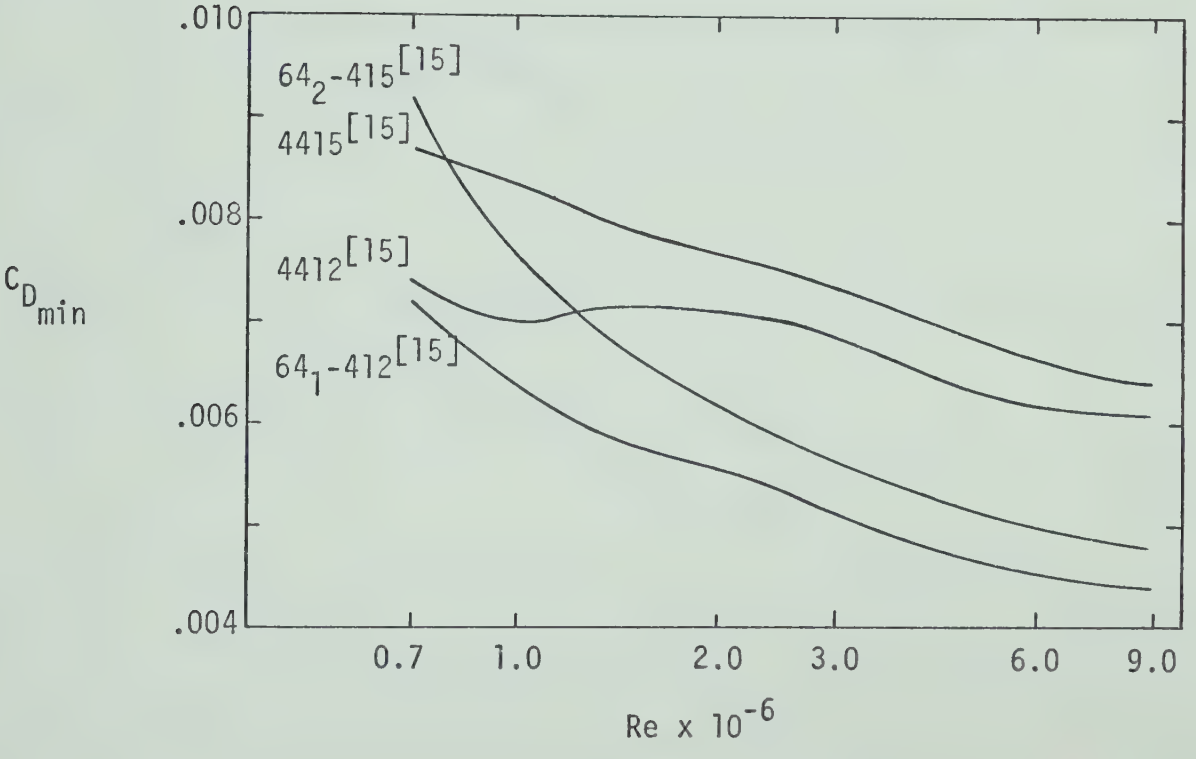

FIGURE 3-1

VARIATION OF $C_{D_{min}}$ AND $C_{L_{max}}$ WITH REYNOLDS NUMBER

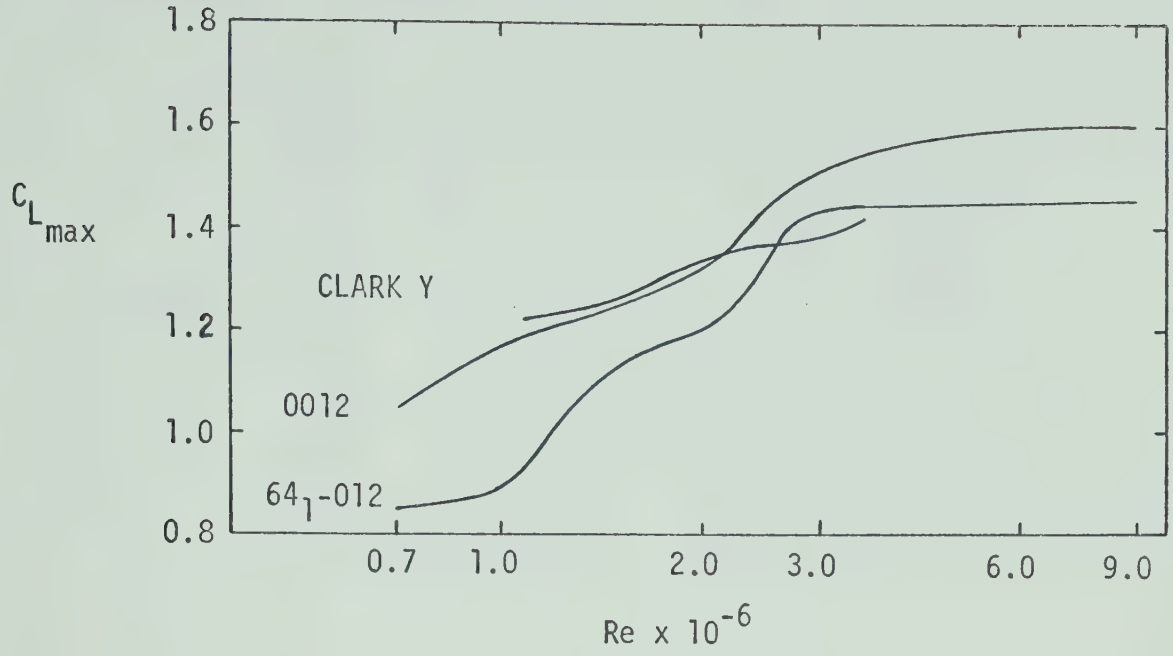

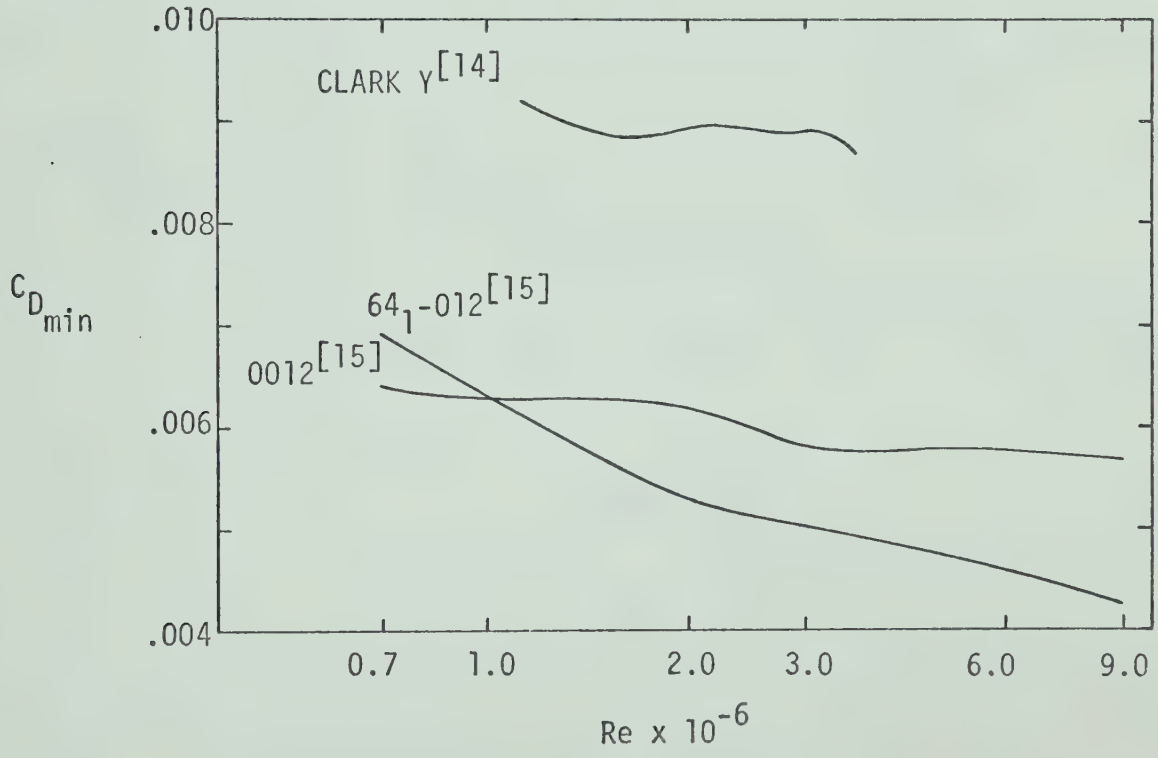

FIGURE 3-2

VARIATION OF $C_{D_{min}}$ AND $C_{L_{max}}$ WITH REYNOLDS NUMBER

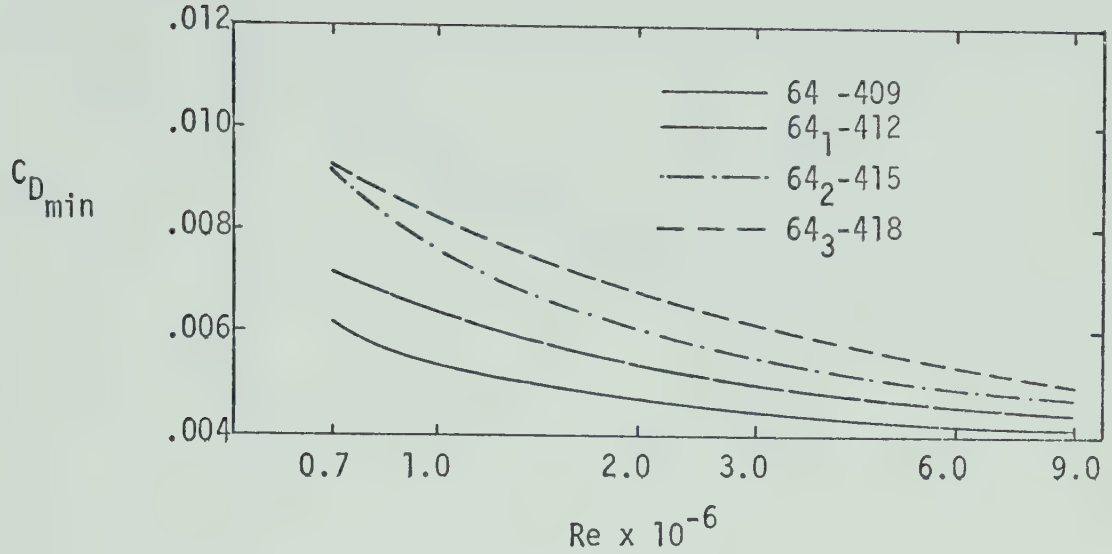

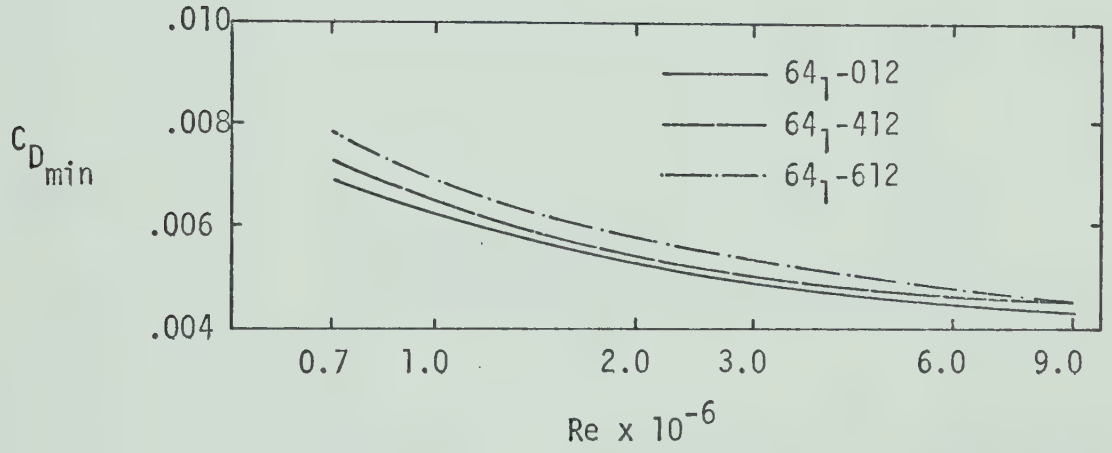

FIGURE 3-3[15]

VARIATION OF $C_{D_{min}}$ WITH REYNOLDS NUMBER

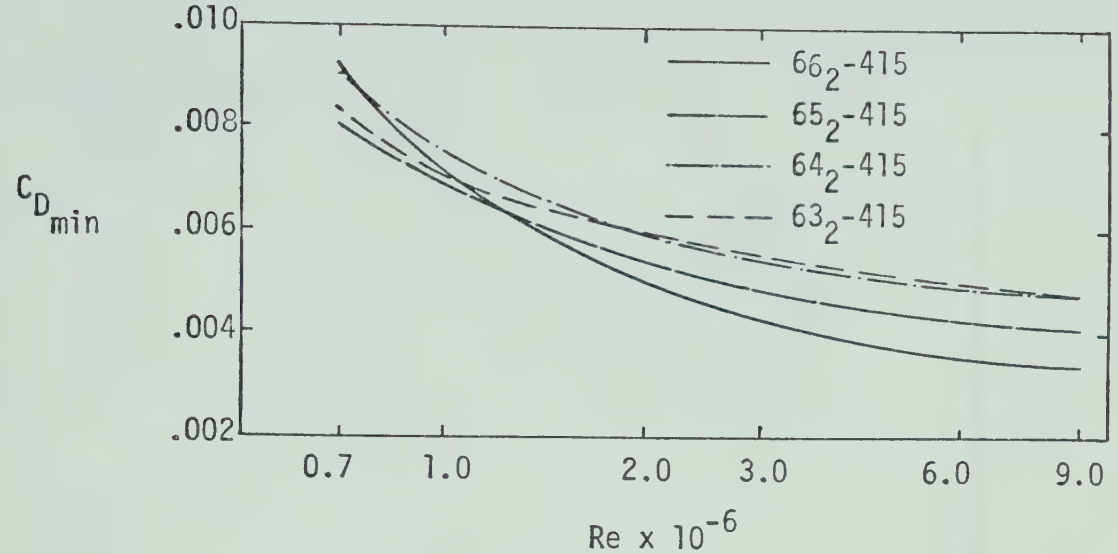

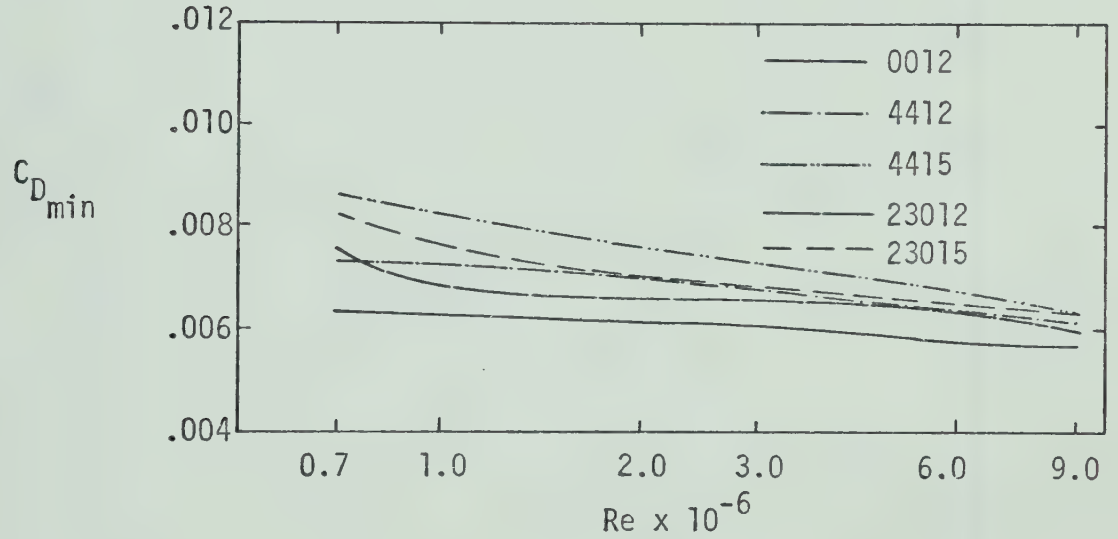

FIGURE 3-4[15]

VARIATION OF $C_{D_{min}}$ WITH REYNOLDS NUMBER

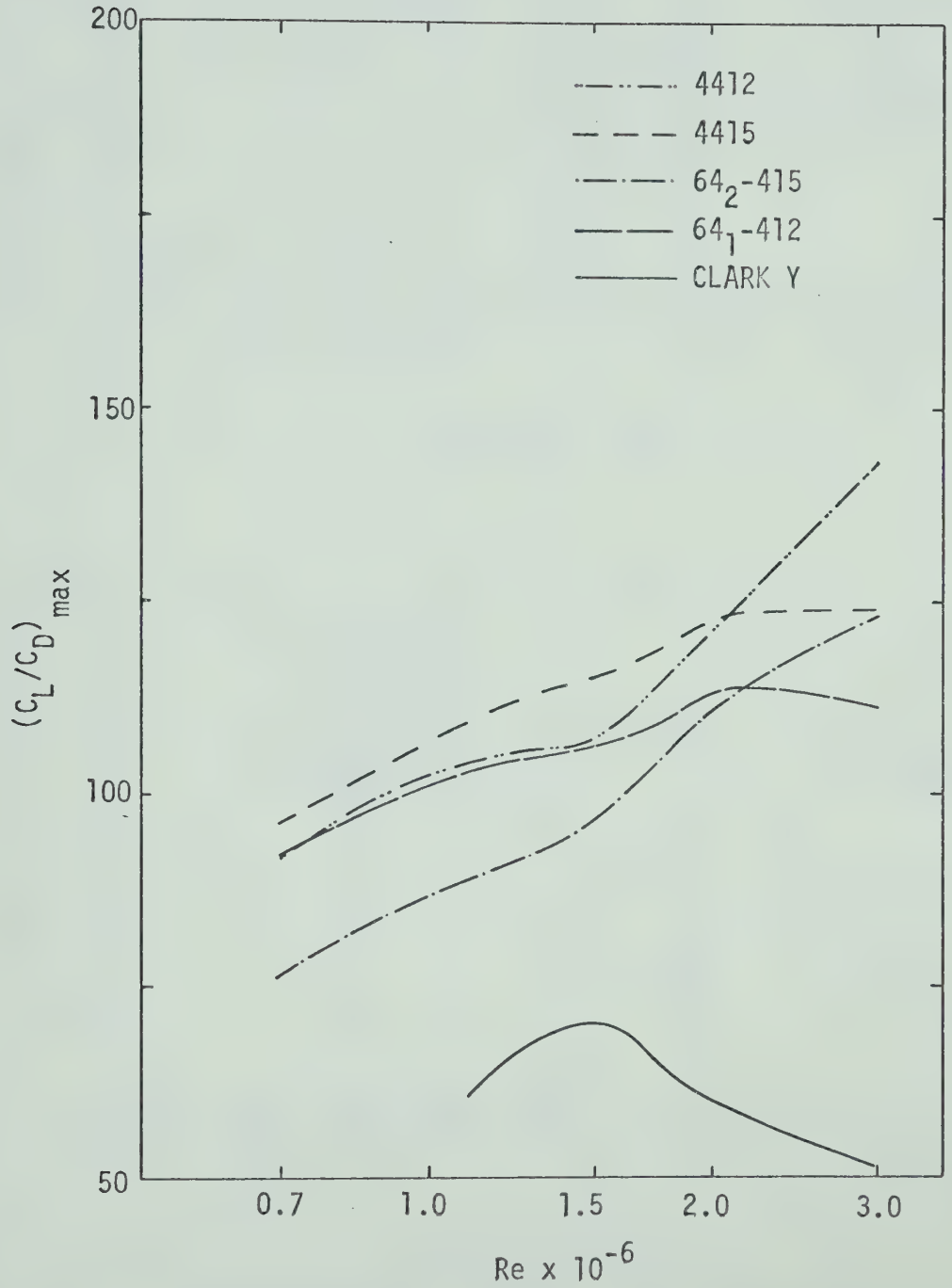

FIGURE 3-5

VARIATION OF $(C_L/C_D)_{max}$ WITH REYNOLDS NUMBER

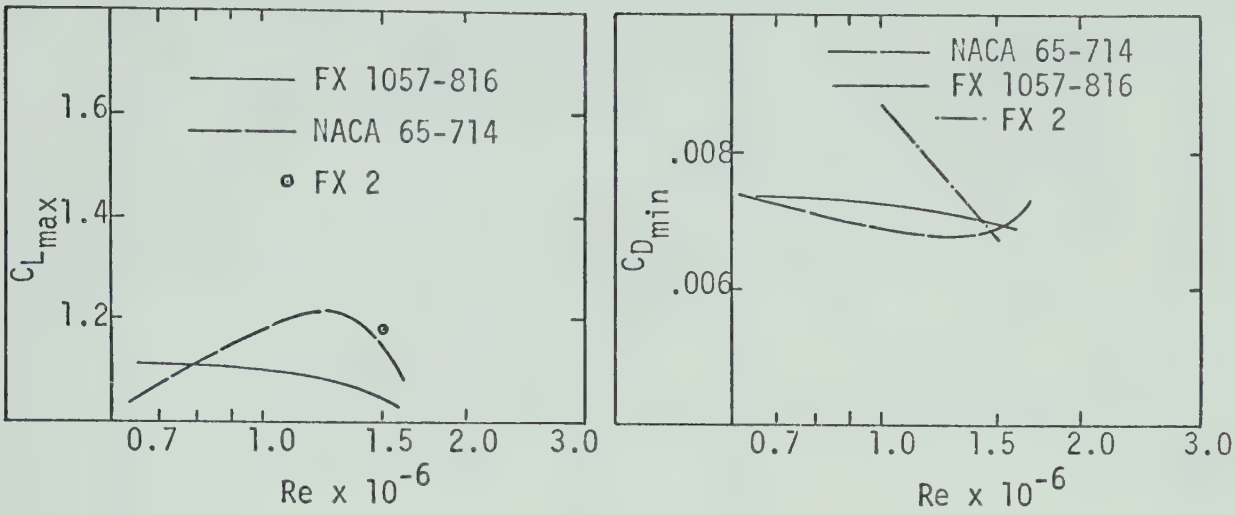

FIGURE 4-1(a)

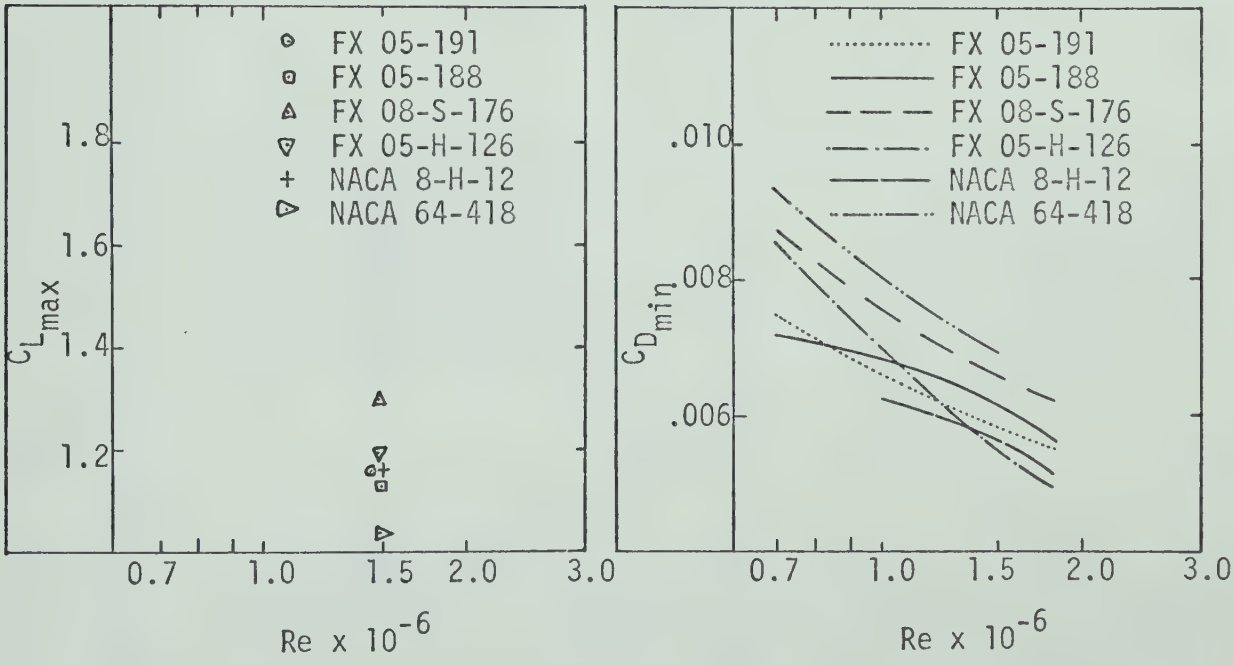

FIGURE 4-1(b)

VARIATION OF $C_{L_{max}}$ AND $C_{D_{min}}$ WITH REYNOLDS NUMBER

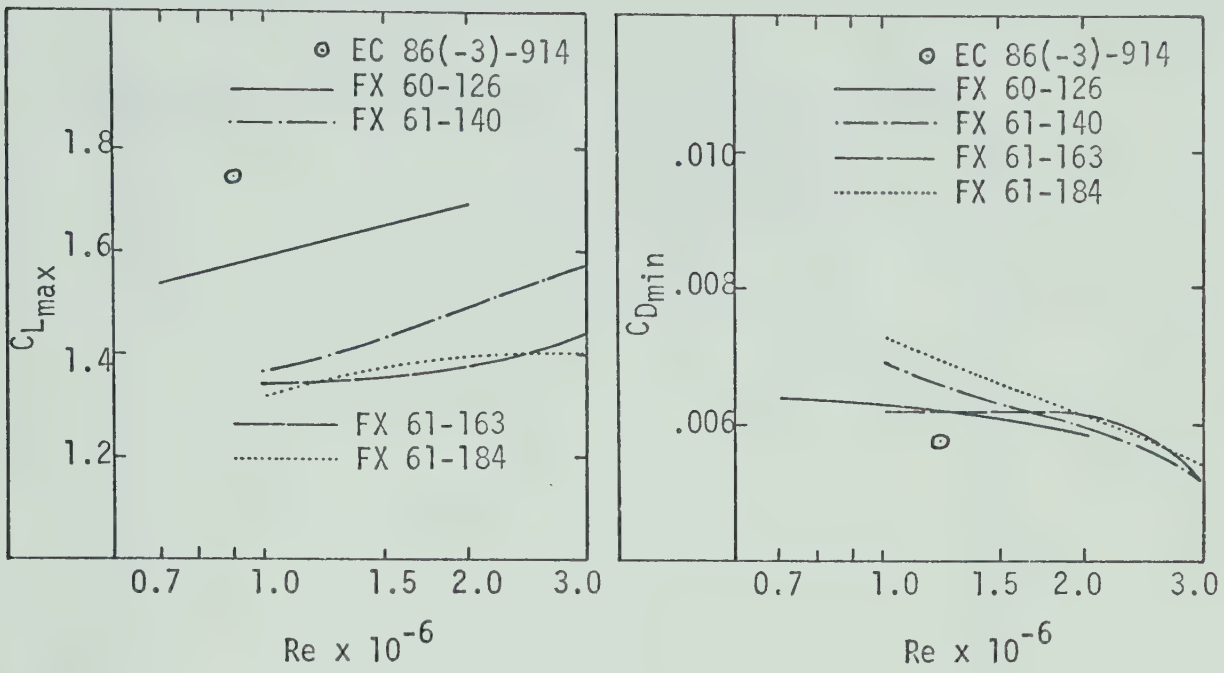

FIGURE 4-2(a)

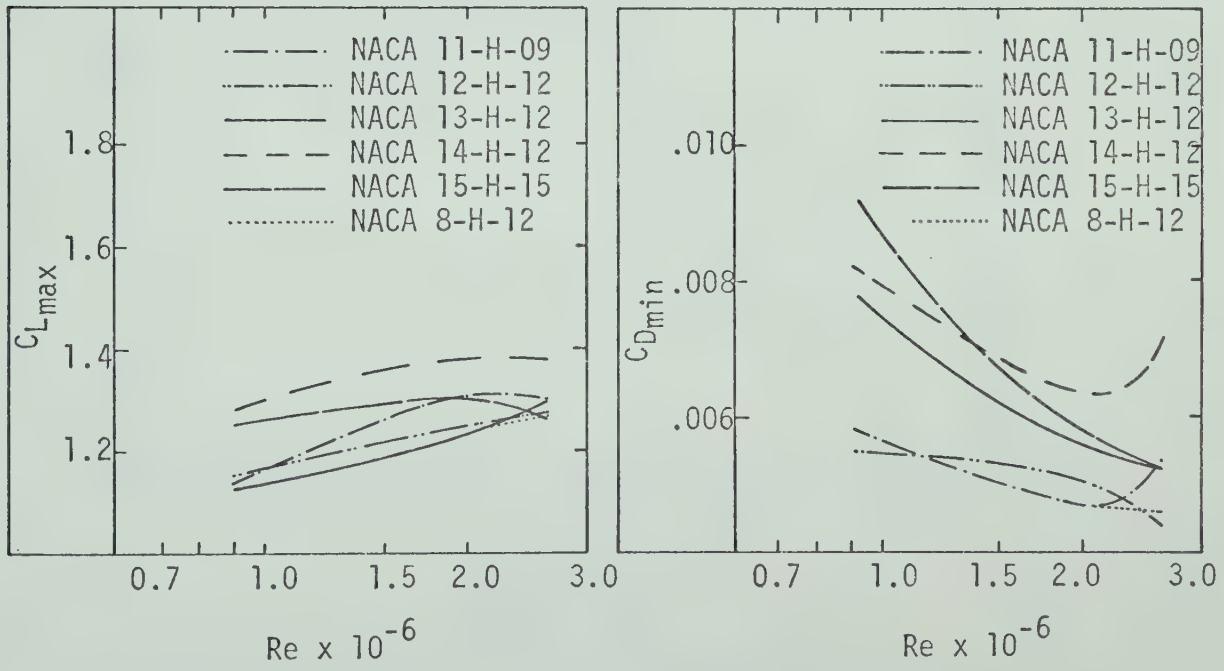

FIGURE 4-2(b)

VARIATION OF $C_{L_{max}}$ AND $C_{D_{min}}$ WITH REYNOLDS NUMBER

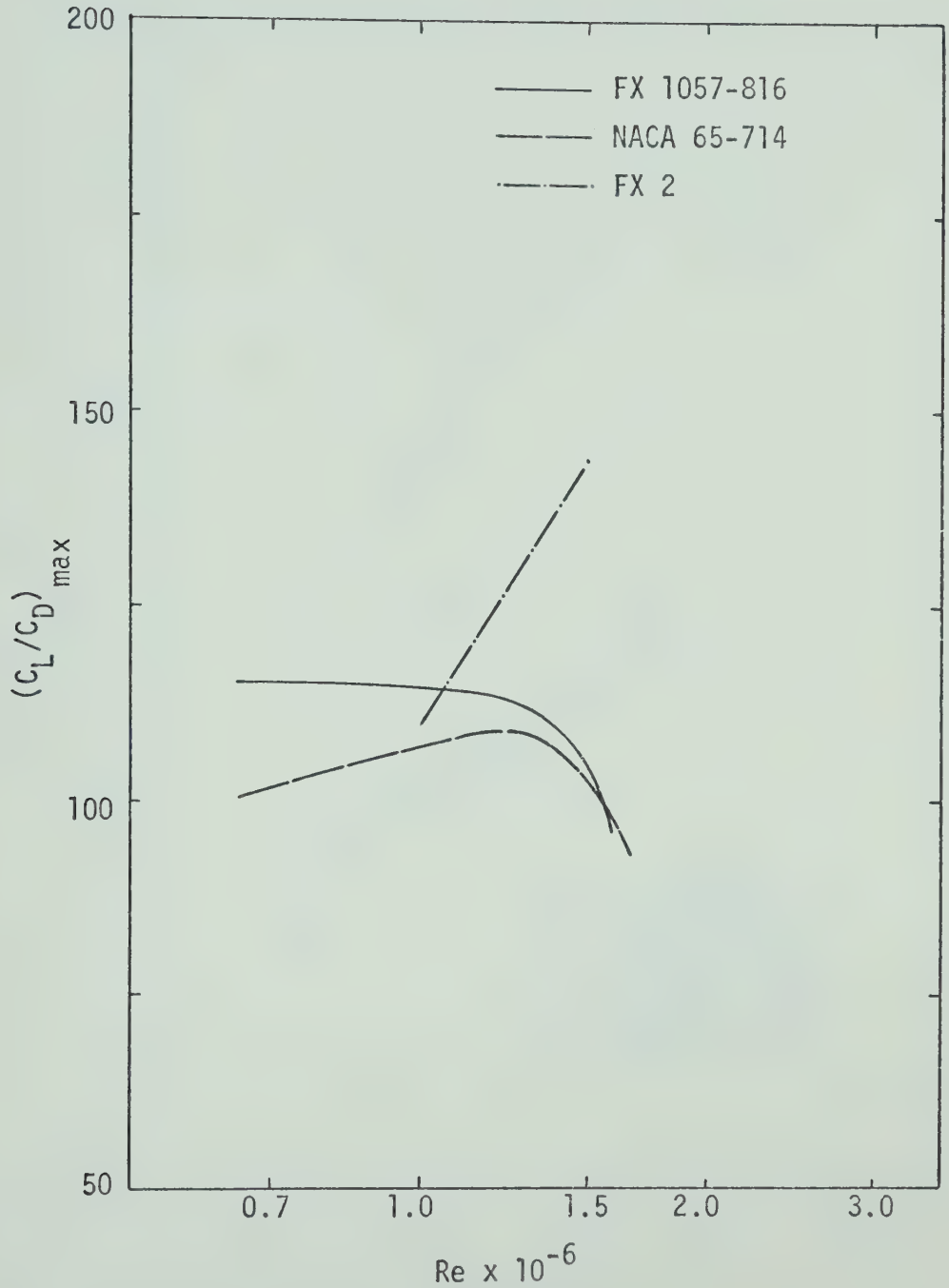

FIGURE 4-3

VARIATION OF $(C_L/C_D)_{max}$ WITH REYNOLDS NUMBER

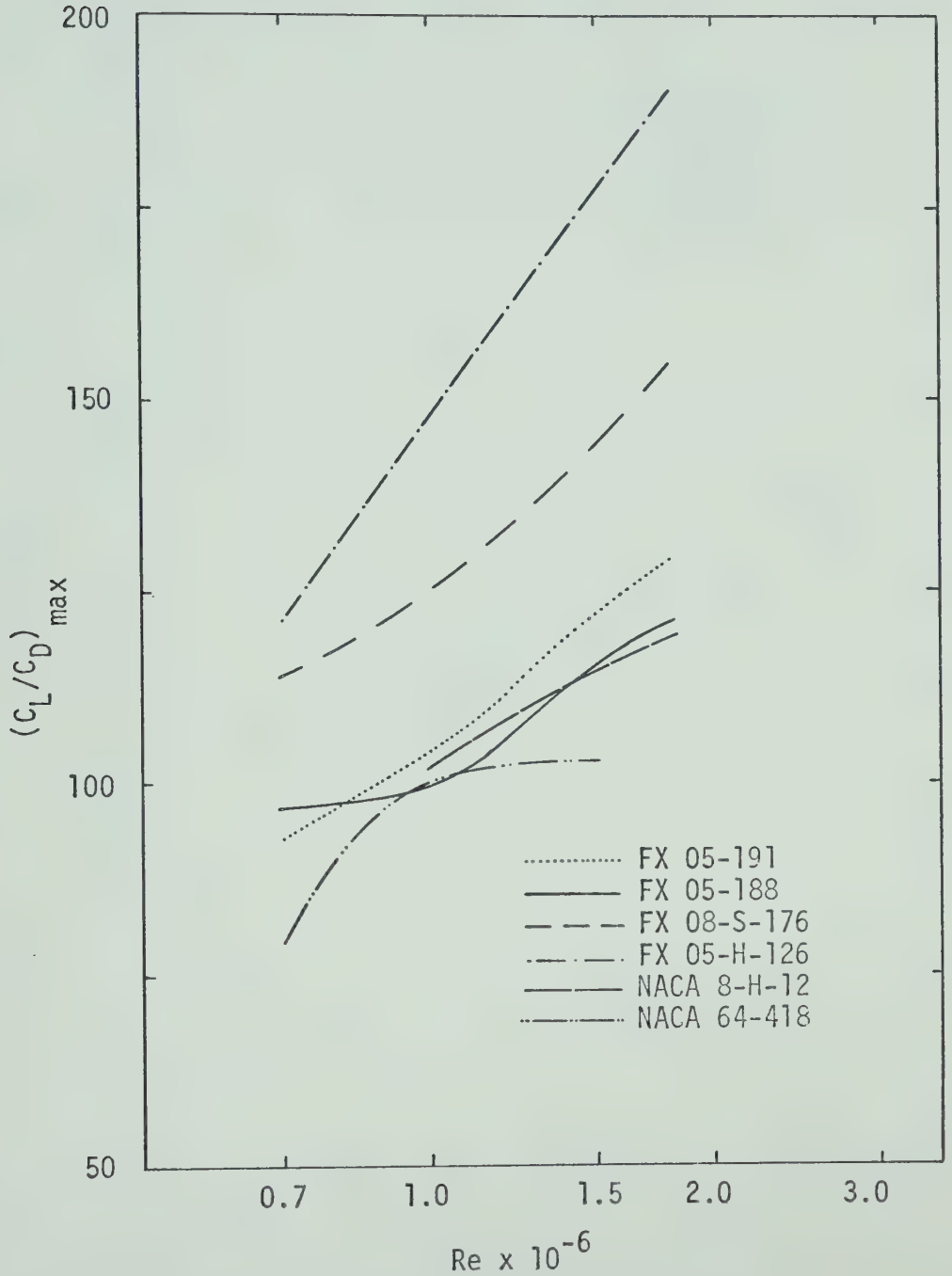

FIGURE 4-4

VARIATION OF $(C_L/C_D)_{max}$ WITH REYNOLDS NUMBER

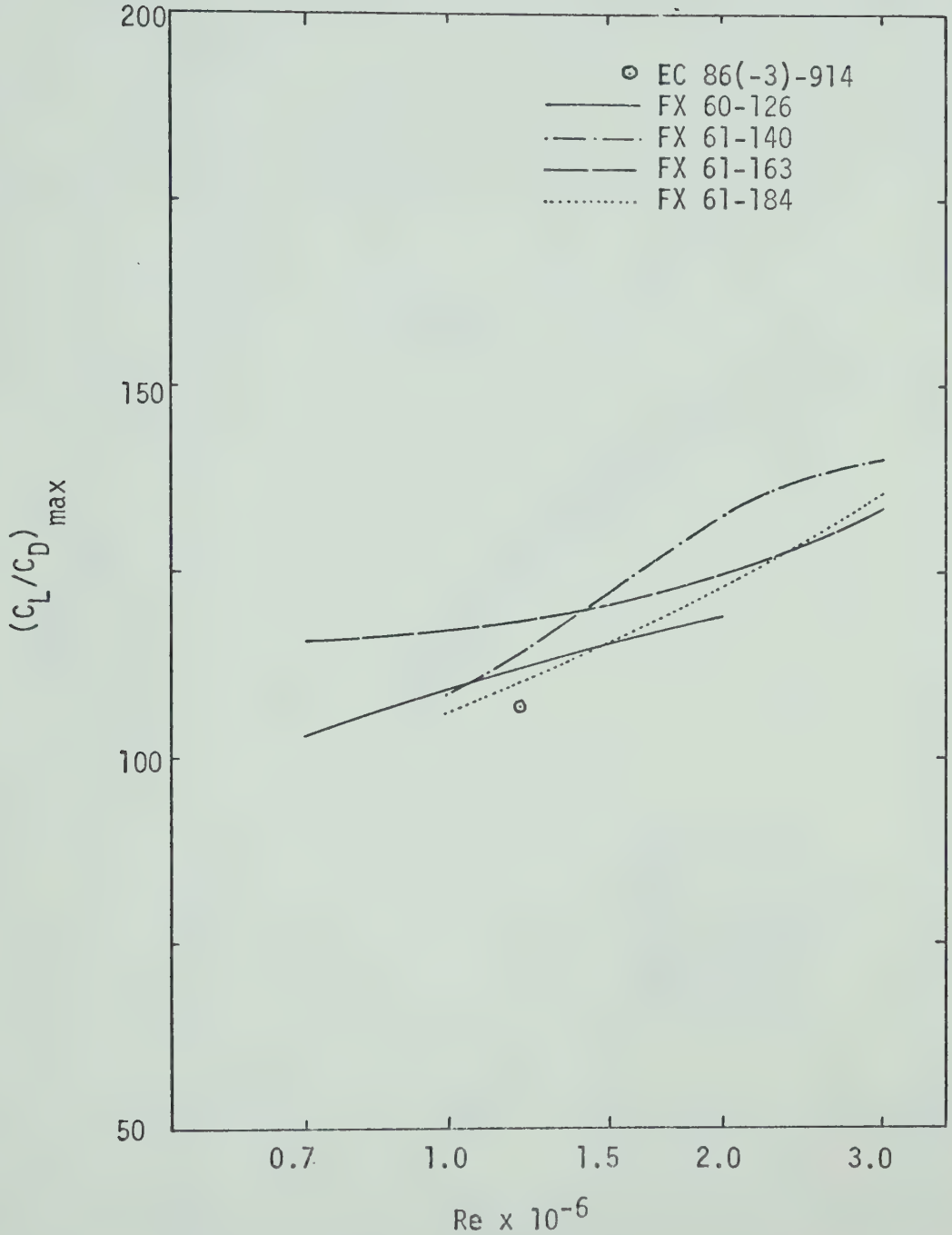

FIGURE 4-5

VARIATION OF $(C_L/C_D)_{max}$ WITH REYNOLDS NUMBER

FIGURE 4-6

VARIATION OF $(C_L/C_D)_{max}$ WITH REYNOLDS NUMBER

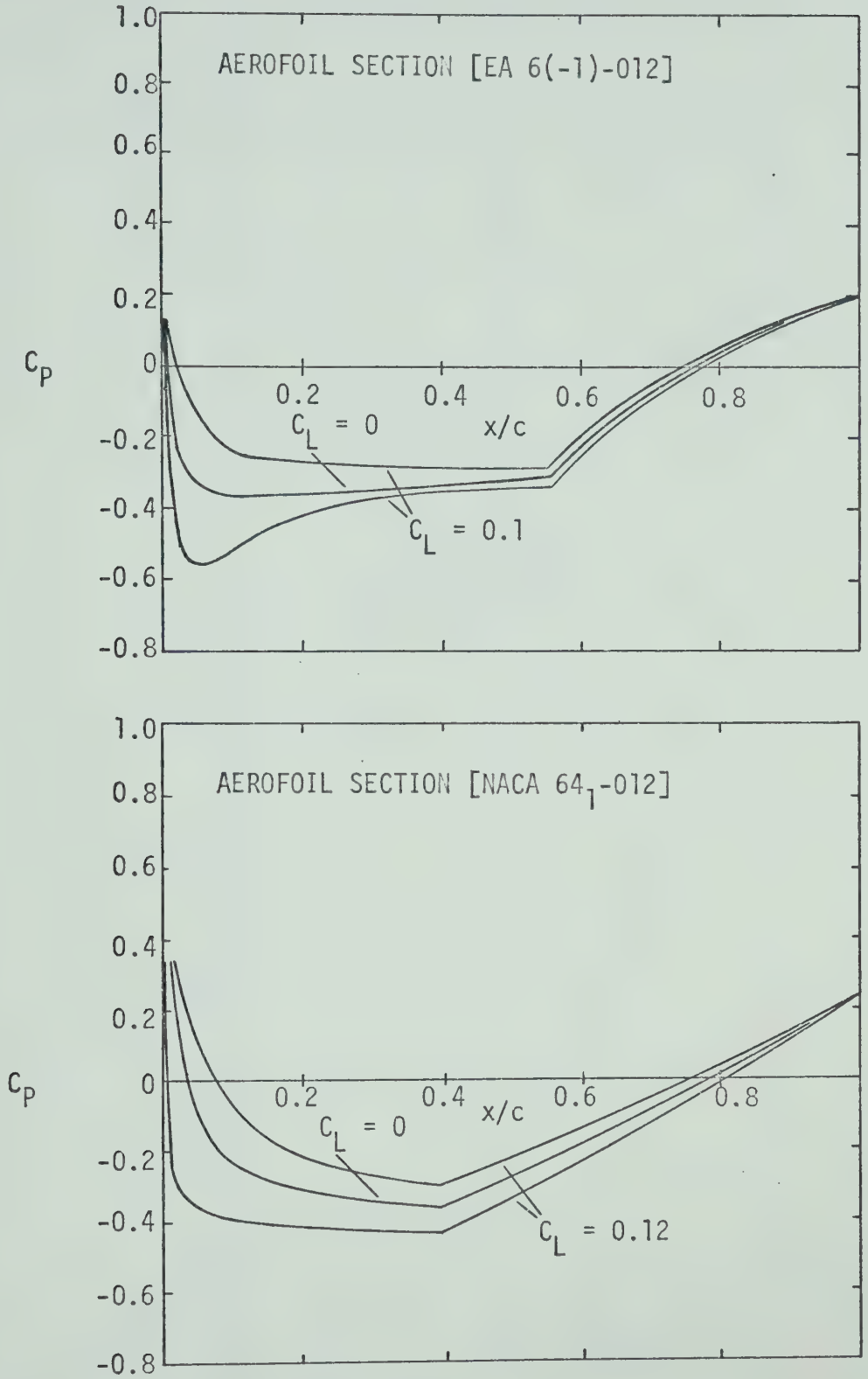

FIGURE 4-7[16]

PRESSURE DISTRIBUTIONS ON TWO AEROFOILS

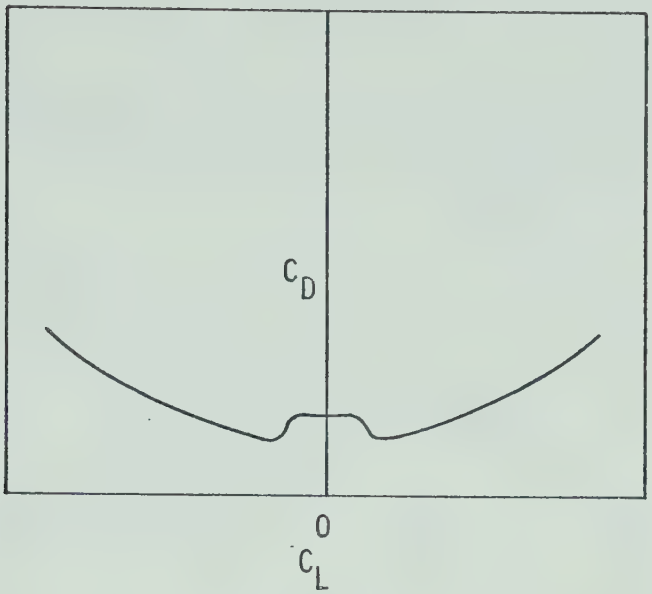

FIGURE 4-8[16]

EXPECTED POLAR DIAGRAM [EA 8(-1)-0...]

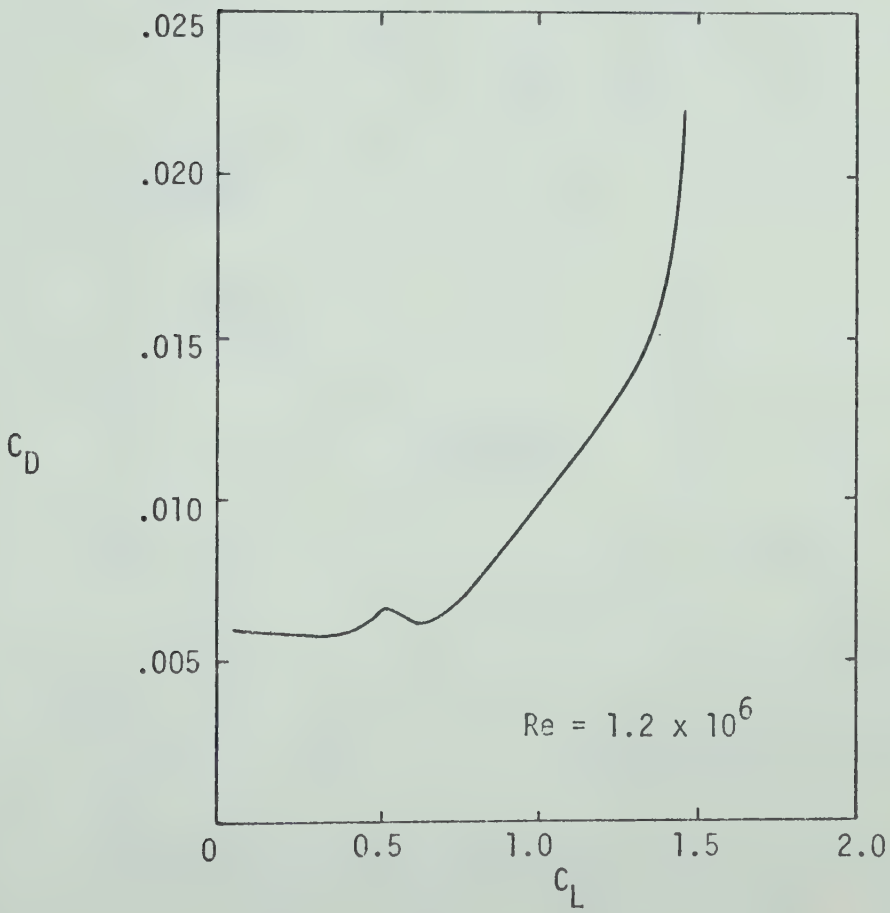

FIGURE 4-9[23]

EXPERIMENTAL POLAR DIAGRAM [EC 86(-3)-914]

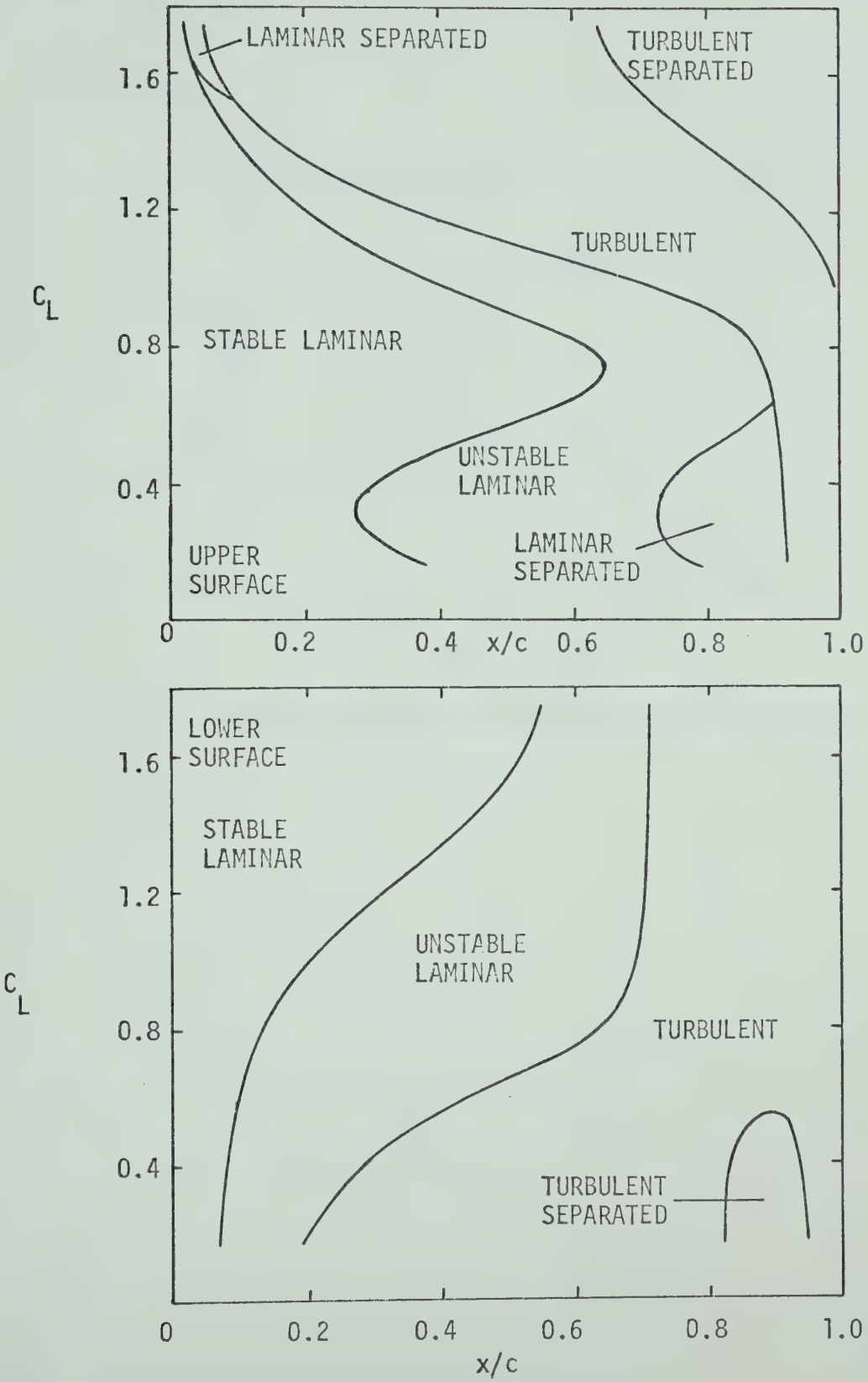

FIGURE 4-10[23]

BOUNDARY LAYER DEVELOPMENT - EC 86(-3)-914

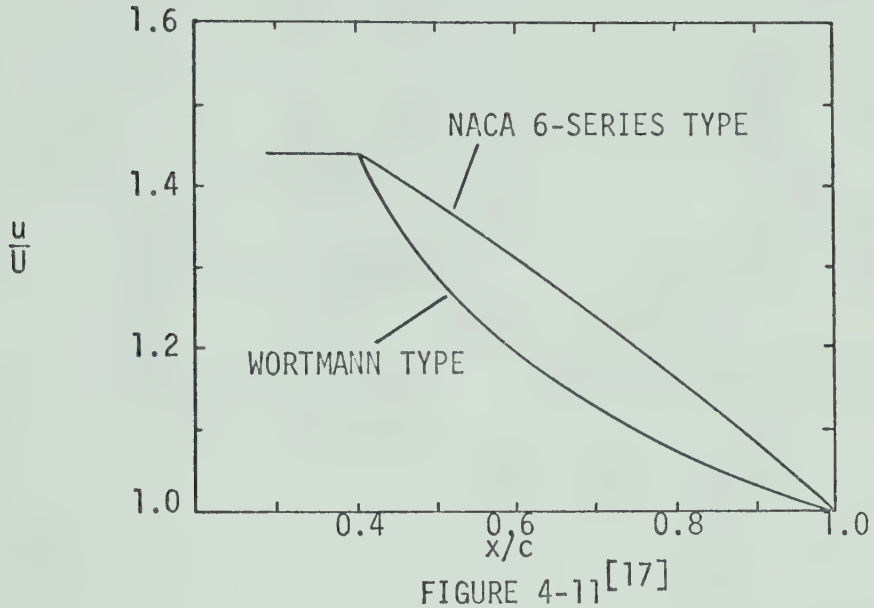

FIGURE 4-11[17]

TYPICAL VELOCITY DISTRIBUTIONS ON TWO AEROFOILS

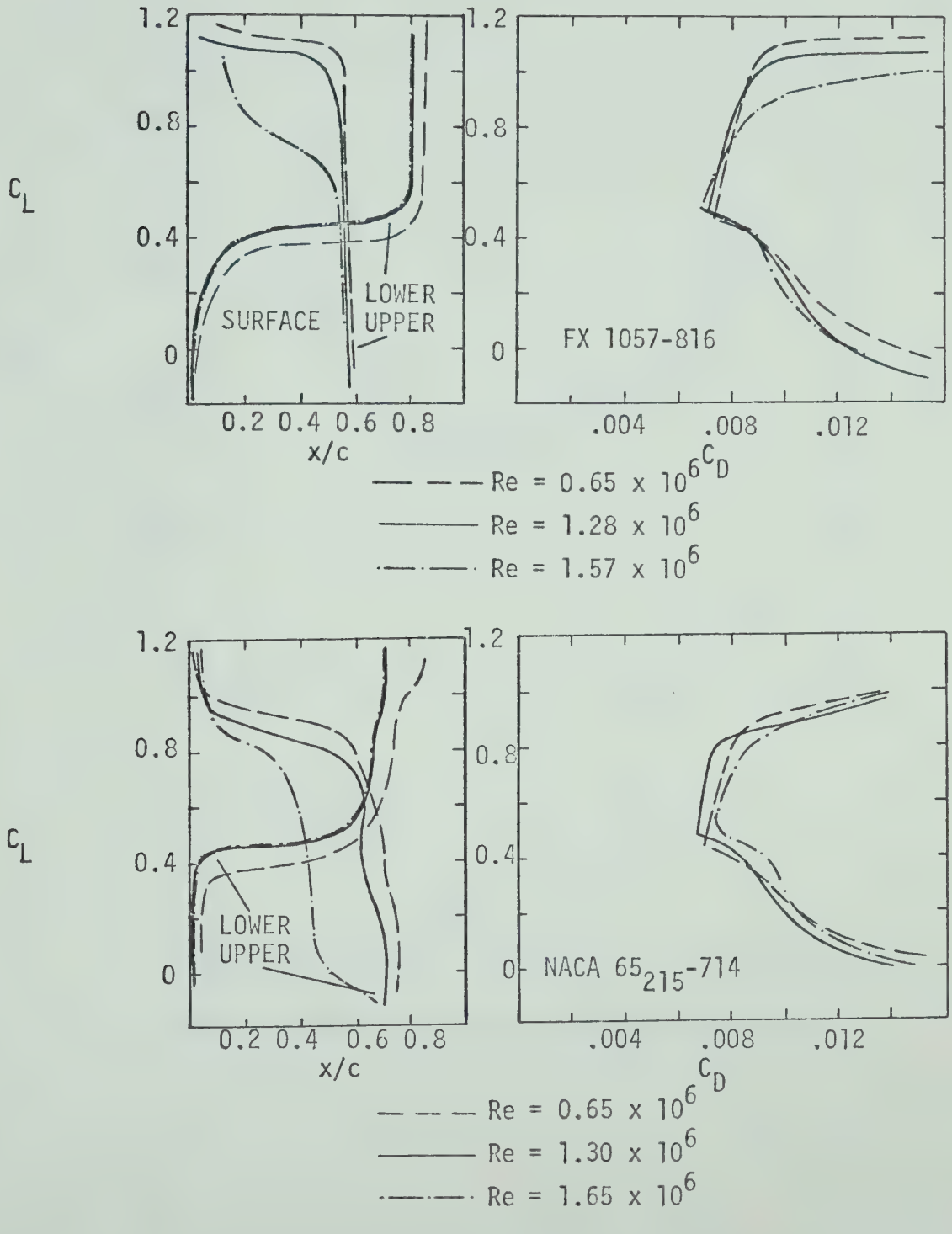

FIGURE 4-12[22]

POSITION OF TRANSITION AND POLAR DIAGRAMS FOR TWO AEROFOILS

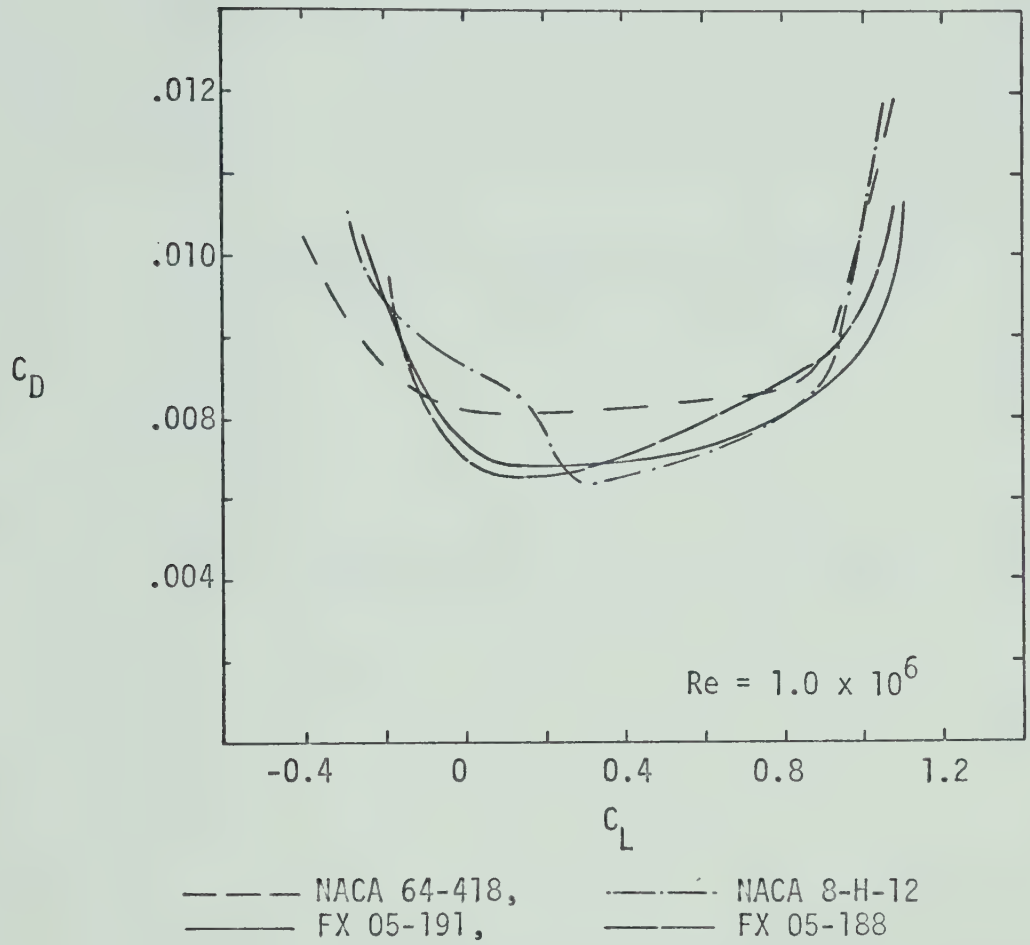

FIGURE 4-13[18]

COMPARISON OF POLAR DIAGRAMS OF TWO CONVENTIONAL AEROFOILS AND TWO LOW REYNOLDS NUMBER AEROFOILS

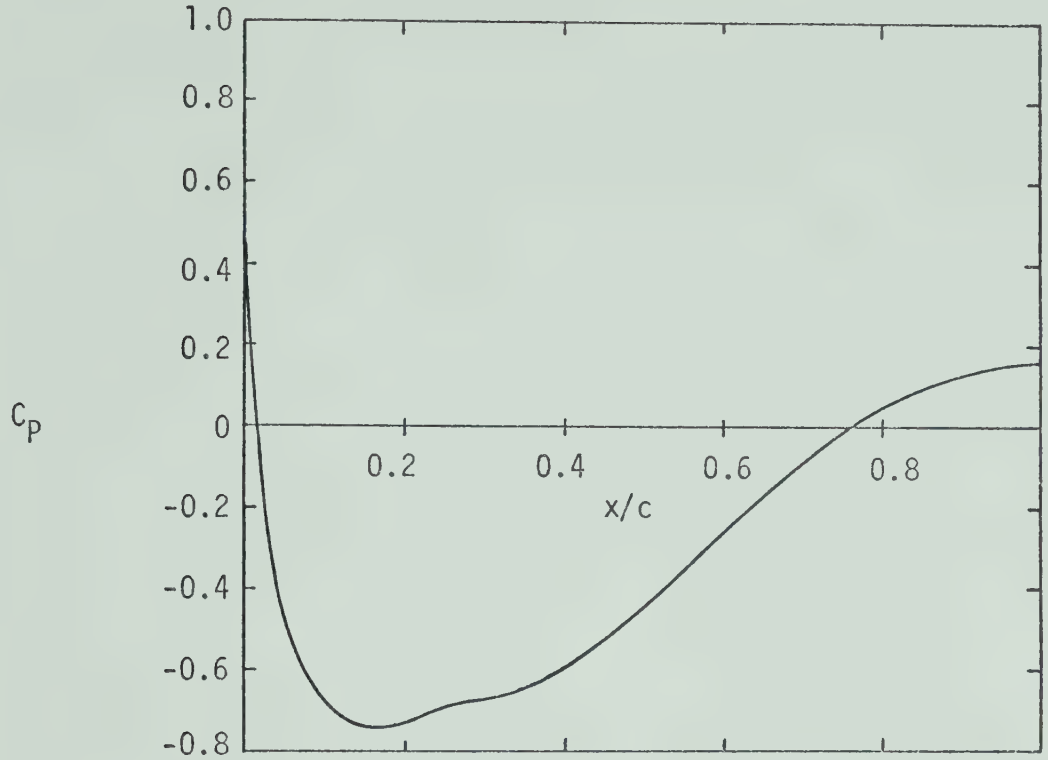

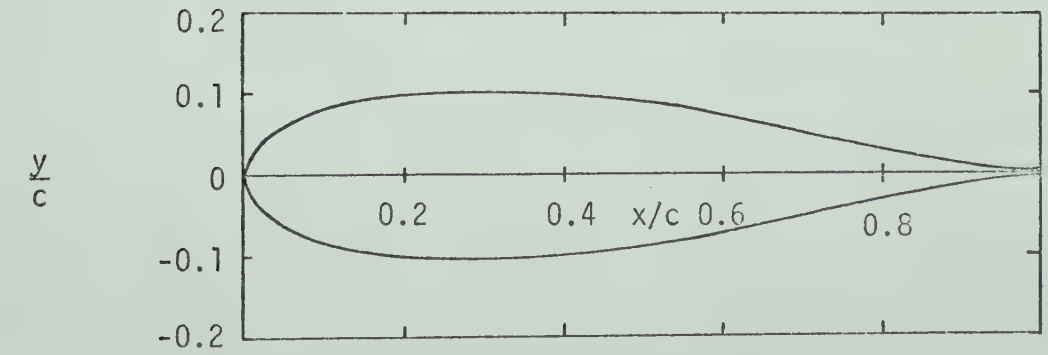

FIGURE 4-14[21]

PRESSURE DISTRIBUTION AND PROFILE

(TAIL FLUKE - COMMON DOLPHIN)